Intelligence 63 (2017) 9–28

Contents lists available at ScienceDirect

Intelligence

journal homepage: www.elsevier.com/locate/intell

Dissecting the parieto-frontal correlates of fluid intelligence: A comprehensive ALE meta-analysis study

Emiliano Santarnecchi[a,*], Alexandra Emmendorfer[a], Alvaro Pascual-Leone[a,b], on behalf of Honeywell SHARP Team authors[a,b,c,d,e]

[a] Berenson-Allen Center for Noninvasive Brain Stimulation, Beth Israel Deaconess Medical Center, Harvard Medical School, Boston, MA, USA
[b] Institut Universitari de Neurorehabilitacio Guttmann, Badalona, Barcelona, Spain
[c] Honeywell Labs, Honeywell Aerospace, Redmond, WA, USA
[d] Electrical and Computer Engineering Department, Northeastern University, Boston, MA, USA
[e] Department of Experimental Psychology, University of Oxford, Oxford, UK

ARTICLE INFO

Keywords:
Fluid intelligence
Abstract reasoning
fMRI
ALE
Functional connectivity

ABSTRACT

Recent advances in cognitive neuroscience have shown how experience-independent cognitive abilities termed fluid intelligence (G*f*) can predict academic achievement, longevity and resilience to neurodegeneration. Therefore, the understanding of the neurobiological underpinnings of G*f* becomes a crucial step for the implementation of cognitive rehabilitation as well as enhancement interventions. Here we present the result of a quantitative meta-analysis of available fMRI and PET literature about G*f* in humans, including (i) distinct maps for verbal and visuospatial stimuli, (ii) an analysis of brain regions contributing to processing of more complex stimuli as well as (iii) a model-driven distinction of processing stages occurring during G*f*-related problem solving. Results highlight the loading of G*f* components over functionally defined resting-state fMRI networks, with different degrees of overlap in both hemispheres and subcortical structures. A major role for nodes of the dorsal attention network during both verbal and visuospatial abstract reasoning tasks represents the most consistent correlate of G*f*, with additional contributions by regions of the anterior salience and left fronto-parietal control network. Increase in trial difficulty elicits a more pronounced engagement of the language and left fronto-parietal control networks, while inferring the rules subtending a given G*f* task relies on a different anatomo-functional substrate than producing novel solutions. Current findings might allow a clearer association between G*f*-related activity and brain connectivity, also providing quantitative ALE maps to be used in network-based brain stimulation and cognitive training interventions.

1. Introduction

Real-life problem-solving tasks require more than a mere access to previously accumulated experience-based information. When challenged with novel situations, the accurate retrieval from long-term acquired knowledge could be useless if new relations between objects are not captured, immediately capitalized, and correct online solutions based on logic promptly extrapolated. Such crucial, experience-independent, components of human cognition –clustered into the term fluid intelligence (G*f*) (Cattell, 1963)–are fundamental in encoding new information efficiently, which can be exploited successfully as a crystallized form of intelligence (G*c*). As a matter of fact, G*f* has been shown to positively correlate with a vast number of cognitive activities, and to be an important predictor of both educational and professional success (Deary, 2008). G*f*, as other cognitive resources, usually declines with physiological aging and, even more, when pathological processes overlap; hence, its decline contributes to the dramatic functional impairment of many chronic-degenerative neurological conditions (Whalley, Deary, Appleton, & Starr, 2004). However, such vulnerability contrasts with the resilience of G*f* towards influences of education, socialization, drug-related interventions (stimulants) and behavioral training (Baltes, Staudinger, & Lindenberger, 1999)(Gray, Chabris, & Braver, 2003), making it a key element for the implementation of effective cognitive neurorehabilitation programs.

The first step for the enhancement of such a core aspect of human cognition is to understand its neuroanatomical and functional substrates. Several pieces of evidence are available, including investigations focusing on correlates of G*f* using voxel-based morphometry (Colom, Chuderski, & Santarnecchi, 2016b; Colom et al., 2013b, 2016a), surface-based morphometry (Escorial et al., 2015), lesion

* Corresponding author
E-mail address: esantarn@bidmc.harvard.edu (E. Santarnecchi).

http://dx.doi.org/10.1016/j.intell.2017.04.008
Received 16 January 2017; Received in revised form 31 March 2017; Accepted 24 April 2017

mapping (Barbey, Colom, Paul, & Grafman, 2014; Barbey et al., 2012), magnetic resonance imaging (MRI) spectroscopy (Nikolaidis et al., 2016; Paul et al., 2016) and functional MRI (fMRI) (Cole, Yarkoni, Repovs, Anticevic, & Braver, 2012; Ebisch et al., 2012; Geake & Hansen, 2005, 2010; Preusse, van der Meer, Deshpande, Krueger, & Wartenburger, 2011). More specifically, neuroimaging and behavioral evidence indicate a limited number of brain areas supporting abstract reasoning abilities: tasks assessing G*f* are usually associated with different levels of frontal and parietal activations (Jung & Haier, 2007)(R. Colom et al., 2013a)(Vakhtin, Ryman, Flores, & Jung, 2014), with parieto-frontal shifts of activity with increasing task difficulty (Houde, 2010); left prefrontal lobe activity has been documented when information is manipulated following perceptual processing involving the parietal lobes (Krawczyk, 2012); additionally, an overlap between visuospatial and verbal analogical reasoning activations in the prefrontal cortices has been proposed, suggesting the existence of a single processing module for distinct modality-specific reasoning tasks (Krawczyk, Michelle, & Donovan, 2011); finally, specific subtypes of logic tasks involving conditional arguments (primarily based on Modus Tollens: e.g. If P then Q; not-Q) seem to map in the prefrontal cortices (mainly left middle frontal gyrus, MFG), while those based on relational syllogisms (e.g. P is to the left of Q; Q is to the left of R; R?) have been linked to the temporo-parietal-occipital junction (Prado, Van Der Henst, & Noveck, 2010). These studies, mostly based on fMRI and positron emission tomography (PET), support the idea of distinct substrates for stimulus types and processing stages. However, their single observation nature limit their value and suggest the need for a comprehensive quantitative meta-analysis of activation patterns during cognitive processing ascribed to G*f*. Most importantly, a detailed characterization of the anatomical substrate of different types of reasoning (e.g. verbal vs visuospatial) across studies is needed, as well as an investigation of brain regions responsible for the different processing stages and those crucially recruited where more challenging trials are faced. Interestingly, the same effort has been put on the definition of similar maps for general intelligence–in the form of intelligence quotient (IQ)—with the conceptualization of the parieto-frontal integration theory (P-FIT) representing a pivotal milestone for the definition of new hypotheses (Jung & Haier, 2007). A similar quantitative understanding of G*f* would help reach a consensus around the localization of such an important feature of human cognition, also offering new insight about potential targets for non-invasive brain stimulation (NIBS) and cognitive training interventions aimed at enhancing cognition (Bestmann, de Berker, & Bonaiuto, 2015). Therefore, we present a quantitative meta-analysis of the G*f* literature available to date, realized analyzing experimental work involving task-fMRI data within the activation likelihood estimate (ALE) statistical framework (Eickhoff, Bzdok, Laird, Kurth, & Fox, 2012; Eickhoff et al., 2009). Quantitative functional mapping for (i) the overall G*f* network, (ii) its verbal and visuospatial components (iii), the different stages of cognitive processing taking place during typical G*f* testing (e.g. rule inference and rule application) and (iv) regions activated during higher difficulty trials, are presented.

Looking at brain spontaneous patterns of metabolic activity might be informative about–and even predict—individual evoked activity during sensorimotor and cognitive tasks (Fox et al., 2005)(Allen et al., 2014; Finn et al., 2015; Shirer, Ryali, Rykhlevskaia, Menon, & Greicius, 2012). Such intrinsic activity is thought to reflect not only the past experiences of the brain as a complex system, but it also forms the functional foundation from which the brain will generate future goal-oriented behavior (Tavor et al., 2016). Differently from canonical task-fMRI paradigm where the signal is derived by contrasting subject's activity during an active and a passive state, this approach relies on the endogenous brain oscillations recorded during spontaneous brain activity, giving rise to a complex pattern of temporally and spatially independent resting-state networks (RSNs)(Biswal et al., 2010). Such intrinsic organization of spontaneous brain activity is captured within the framework of brain connectivity analysis, an approach based on resting-state fMRI analysis (Achard & Bullmore, 2007). Individual connectivity profile has been proven reliable over multiple sessions (Braun et al., 2012)(Choe et al., 2015), and to hold enough information not only to allow the identification of pathological conditions (e.g. multiple sclerosis (Bonavita et al., 2016), schizophrenia (Bassett et al., 2008) and Alzheimer (Agosta et al., 2012)) but also to identify correlates of several cognitive (Santarnecchi, Galli, Polizzotto, & Rossi, 2014)(Santarnecchi, Rossi, & Rossi, 2015b; Santarnecchi, Tatti, Rossi, Serino & Rossi 2015c; Yuan et al., 2012) and psychological traits (Adelstein et al., 2011) in healthy subjects. However, a clear overview of the role played by regions activated during G*f* tasks with respect to existing RSN is not available to date, with potential insight coming from the P-FIT model suggesting a major role for regions of an anatomically defined "fronto-parietal network". To provide such information, we quantitatively compared each G*f* map with those representing different RSNs tapping into domains such as attention, executive control, language, sensorimotor, visual and auditory processing. Results provide an original overview of the link between G*f*-related brain activity and brain functional connectivity in humans.

2. Methods

2.1. Literature search

Potentially relevant articles were retrieved by performing a search in PubMed and Google Scholar database without temporal restrictions. The following terms were individually combined with "functional magnetic resonance imaging", "Position Emission Tomography" and their acronyms: "Fluid intelligence", "G*f*", "abstract reasoning", "logical reasoning", "rule inference", "rule application", "divergent thinking" "convergent thinking", "deductive reasoning", "analogical reasoning", "relational processing", "inductive reasoning", "syllogistic reasoning", "inductive reasoning", "conditional reasoning". References of retrieved researches were examined for relevant publications too. We intentionally excluded (i) studies including patients with organic illness, (ii) studies discussing magic ideation, (iii) review papers, (iv) studies not mentioning any of the keywords in their abstract unless they cite specific G*f* related tasks, (v) studies not reporting fMRI/PET activations coordinates in MNI or Talairach space, (vi) studies using a-priori defined regions of interest, (vii) studies not reporting activation foci in table format or reporting statistical values without corresponding coordinates.

The final selection comprised 47 studies related to fMRI and PET (see Supplementary Table S1). For each study, the following information was retrieved: (i) number of participants, (ii) mean age, (iii) experimental design, (iv) cognitive task parameters, (v) main results. Data for each specific activation foci have been also collected and included in a quantitative Activation Likelihood Estimation (ALE) analysis for the identification of brain regions most commonly reported as involved in G*f* processing. Different maps were created, carefully inspecting each manuscript and extracting activation foci from tables referring to the contrast of interest. As a result, a (1) global "G*f*" map was obtained by including all the coordinates referring to G*f*-related processing, regardless the stage of processing and stimulus type; a (2) "verbal" and a (3) "visuospatial" G*f* maps (vG*f* and vsG*f* hereafter) were computed by including studies using verbal stimuli such as analogies, or visuospatial ones such as Raven matrices (Raven, Raven, & Court, 1998); more specifically, vG*f* refers to studies using written text as part of the experimental stimuli (words, letters, numbers, or any other type of stimuli requiring a stimuli-dependent semantic process), in the context of tasks based on, for instance, analogies (Luo et al., 2003), induction (Green, Fugelsang, Kraemer, Shamosh, & Dunbar, 2006) and syllogistic reasoning (Goel, Buchel, Frith, & Dolan, 2000); differently, studies using original or modified version of well-known G*f* measures such as the Raven's Advanced Progressive Matrix test (Raven et al.,

1998), Sandia (Matzen et al., 2010) and Bomat tests (Hossiep et al., 1999) , were considered as indexing vsG*f*, together with studies using ad-hoc stimuli based on geometrical figures of different colors, shape, dimension, with no requirements for explicit semantic processing (e.g. reading a premise) during any processing stage.

As for rule inference (RI) and rule application (RA), only a subsample of the studies analyzed included a distinction between the two processing stages. Where the rationale of the study was to specifically investigate processing stages (e.g.(Reverberi et al., 2007, 2010)(Cocchi et al., 2014) information was retrieved following the structure included by the authors; otherwise, a thorough analysis of each paper was done and activation foci were retrieved for trials related to inferring the working principle of the stimuli at hand (e.g. the square seems to precede the triangle in most of the rows; when that is the case, the circle is blue) and corresponding activation foci were labeled as RI; trials where a newly inferred rule was then applied to novel stimuli (e.g. select where the blue circle is supposed to be in a similar array of stimuli, based on the same square/triangle/circle elements as mentioned above) were labeled as RA. Finally, studies reporting results for various levels of stimuli difficulty were also considered (e.g. (Cocchi et al., 2014; Golde, von Cramon, & Schubotz, 2010; Christoff et al., 2001), and activation foci for most difficult trials were extracted and labeled higher complexity (HC). Separate ALE maps were created for each selection of studies/results. For details about the ALE map computation see the dedicated section below.

2.2. ALE map computation

The quantitative evaluation of spatial fMRI patterns was carried out using the activation likelihood estimate (ALE) technique implemented in the GingerALE software v2.3.2 (www.brainmap.org) (Eickhoff et al., 2009; Eickhoff et al., 2012). The method yields a statistical map that indicates the set of brain voxels that are more active than would be expected by chance. Differently from within-study SPM analysis where every voxel in the image space is tested against a null hypothesis of no activation, the ALE method assumes that for each study of interest there is a given spatial distribution of activity and an associated set of maximal coordinates. Therefore, the algorithm tests to what extent the spatial locations of the activation foci correlate across independently conducted fMRI studies investigating the same construct.

First, the lists of coordinates were carefully checked for duplication of data across publications, in order to avoid artefactual inflation of a given foci significance. Coordinates collected from studies reporting activation foci in Talairach space were converted into the MNI space using the tal2mni algorithm implemented in GingerALE. Activation foci from each study were modeled as Gaussian distributions and merged into a single 3D volume. The ALE algorithm modeled spatial uncertainty of each activation focus (Turkeltaub et al., 2012), using an estimation of the inter-subject and inter-study variability usually observed in neuroimaging experiments, rather than applying an apriori full-width half maximum (FWHM) kernel. Therefore, the number of participants in a given study influenced the spatial extent of the Gaussian function used. We first modeled the probability of activation over all the studies at each spatial point in the brain, returning localized "activation likelihood estimates" or ALE values. Values were then compared to a null distribution created from simulated datasets with randomly placed foci, in order to identify significantly activated clusters (permutations test = 1000 run). Following Eickoff and colleagues arguments supporting a better balance between sensitivity and specificity for Cluster-based corrections over False-Discovery-Rate (FDR) and Family Wise Error (FWE) approaches (Eickhoff et al., 2012), we applied cluster correction for multiple comparisons with a $p < 0.001$ threshold for cluster-formation and a $p < 0.05$ for cluster-level inference. Only clusters with a size exceeding the cluster size recommended by ALE were reported (range 500–1000 mm3). Given the potential overlap of the different ALE maps (e.g. vG*f* and vsG*f*, RI and RA), specific statistical comparisons have been computed in order to identify segregated neurobiological signatures of each component as well as conjunction maps showing significant overlaps. The procedure involves the creation of a combined map including the two maps of interest (i.e. including all the activation foci), using the voxel-wise minimum value of the input ALE images. Then, two contrast images are created by directly subtracting the two ALE maps, together with a map showing their statistically significant overlap. It is important to notice that the resulting subtraction image does not take into account differences in the dataset sizes between the two original maps. Therefore, simulated datasets are created by pooling all the available foci and randomly dividing them into two groupings with the same sizes as the original datasets. An ALE image is created for each new dataset, subtracted from the other and then compared to the real data. The process is computed 10,000 times, and a voxel-wise p value image is obtained. Values in each voxel represent the position of real data with respect to the distribution of values obtained during the permutation test. To ease the comprehension of the results, ALE contrast images are converted to Z scores.

This procedure was applied to each of the aforementioned coordinate lists. Results are then express as clusters of activation using Z score values in the image statistics and maxima value. Anatomical labels of final cluster locations were provided by the Talairach Daemon (http://www.talairach.org/daemon.html). ALE maps were visualized using MriCron (Rorden & Brett, 2000) on an MNI standard brain. Moreover, in order to provide anatomical mapping of activation foci according to the recently developed new multimodal parcellation of the human brain (Glasser et al., 2016), ALE volumetric maps have been converted to surface space and overlap to the new atlas using Connectome Workbench software.

2.3. Overlap between Gf and resting-state fMRI networks

Binary spatial maps of RSNs were used to perform spatial mapping of each G*f* ALE map. Networks were defined following the scheme by Shirer et al. (2012), defining 14 non-overlapping maps: the dorsal and ventral default mode (vDMN, dDMN), right and left executive control (RECN, LECN), the dorsal and ventral attention (AN), anterior and posterior salience (AS, PS), basal ganglia (BG), language (LANG), high and primary visual (HVIS, PVIS), precuneus (PREC), auditory (AUD) and somatosensory (SM) networks (Shirer et al., 2012). The total number of voxels composing each ALE map was calculated and then used to estimate the amount of overlap (expressed as percentage value) between each G*f* map and any RSNs. Results were expressed as percentage of each G*f* map area (in voxels).

It should be noted that that different approaches for extracting and labeling RSNs have been applied in different research groups over the last 15 years. For instance, we here consider the AS as a network including bilateral insula (mostly referring to its anterior part) and dorsal anterior cingulate cortex (dACC); according to the work by Dosenbach and colleagues, the same network, with the inclusion of two anterior frontal regions corresponding to Brodmann area 9/10, is also known as the cingulo-opercular network. Both nomenclature refer to a network associated with several executive functions, such as rule maintenance (Bunge et al., 2005), error-related activity and performance monitoring (M. Botvinick, Nystrom, Fissell, Carter, & Cohen, 1999; Carter et al., 1998; M. M. Botvinick, Cohen, & Carter, 2004). The same applies to the LECN and RECN, indicating two lateralized networks resembling the fronto-parietal control network as originally described by the same group (Dosenbach, Fair, Cohen, Schlaggar, & Petersen, 2008; Dosenbach et al., 2007). Both definitions, with the additional distinction of a left and right component in Shirer et al. (2012), refer to a network involved in cognitive control, with a specific involvement in control initiation, flexibility and modulation of response to feedback. Similarly, the AN identified here reflects the ventral and dorsal attention network proposed by Corbetta et al., with

no differentiation between a dorsal (including bilateral parietal lobe, frontal eye fields and, to a lesser degree, parieto-occipital regions) and a ventral component (i.e. more frontal, including regions of the inferior and middle frontal gyrus) (Corbetta, Patel, & Shulman, 2008). This network is involved in attention-related processing, playing a major role in both top-down endogenous control of attention (dAN) and stimulus-driven reorienting (vAN) (Corbetta et al., 2008). Given the very high degree of overlap for the definition and anatomical localization of AS, AN and L/RECN across research groups, we will refer to these labels assuming the same conclusions are applicable to the cingulo-opercular network, ventral and dorsal attention networks and FPCN, discussing relevant difference where needed. Finally, another classification has been proposed by Yeo et al. (2011), including multiple labeling solutions acknowledging the existence of 7 as well as 17 resting-state fMRI networks. The main difference with respect to the work by Shirer et al. (2012) concerns the labeling of a subset of prefrontal regions, classified as part of the FPCN by Yeo et al. (2011) instead of AN (Shirer et al., 2012; Yeo et al., 2011). A graphical representation of both solutions and their differences is included in Fig. 8, where G*f* mapping on both labeling approaches is discussed as part of the Discussion section.

3. Results

3.1. ALE maps

For sake of synthesis, the lists of regions representing each map are presented in separate paragraphs. Detailed information about anatomical localization of each significant cluster and the relative statistics are reported in dedicated figures and tables. A more in-depth discussion about the meaning of the patterns identified as well as the role of specific regions is provided in the discussion section. Each map is available for download as a nifti. nii volumetric file at (http://www.tmslab.org/santalab.php). Both full network and single node level maps are provided, along with corresponding cluster size, coordinates in MNI space and anatomical labeling. Therefore, each node can be used as a stand-alone region of interest for functional connectivity analysis, whereas the entire network map can be used to investigate connectivity patterns with respect to existing RSNs or other brain regions.

3.1.1. Overall Gf and higher complexity trials.

The resulting map and coordinates for the overall pattern of activation during G*f* tasks is reported in Fig. 1 and Table 1. The map includes 16 separate clusters (i.e. nodes) highlighting a bilaterally distributed functional organization mainly involving (left) prefrontal and parietal lobes, with additional contribution from occipital regions and subcortical structures including globus pallidus, thalamus, putamen and insula.

Map and coordinates for the higher complexity trials are reported in Fig. 2 and Table 2. While a bilateral fronto-parietal activation pattern is clearly visible when all trials are summed together, a more localized activation characterizes more challenging trials, with activation of regions placed mostly in the bilateral prefrontal lobe, anterior cingulate cortex and bilateral temporo-occipital junction. Consistent with many reports on left hemispheric involvement in logical reasoning (Prado et al., 2010), higher complexity trials (i.e. those requiring the application of two–or even more—logical operations at the same time, instead of low cognitively loading trials involving single, serial operations) showed increased activation of left prefrontal structures, including the left inferior frontal lobe and the frontal eye fields.

3.1.2. Verbal and Visuospatial Gf

Map and coordinates for the activation pattern elicited during the solution of vG*f* and vsG*f* tasks are shown in Fig. 3 and Table 3. A more left-lateralized activation involving the inferior frontal lobe is visible for vG*f* tasks, while activations of left visual cortex and bilateral frontal eye fields (FEF) are visible for visuospatial tasks. Given the lower number of studies for each stimuli type, resulting maps tend to be smaller than the average G*f* map shown in Fig. 1. In order to capture statistically significant difference between the two reasoning modalities, a statistical comparison of vG*f* and vsG*f* maps has been computed using permutation-based statistics, resulting in the statistical map and set of coordinates reported in Fig. 4 and Table 4. Results show a specific role for ACC and left inferior frontal lobe for verbal stimuli, while regions of the bilateral FEF are more selectively responsible for the processing of vsG*f* assessment. Modality independent regions activated for both stimuli have been identified in the inferior and middle frontal lobes as well as the inferior parietal lobule.

3.1.3. Rule inference and rule application

Activations during RI and RA processing steps and their respective sets of coordinates are reported in Fig. 5 and Tables 5 & 6. A clear distinction between the two processes is present. While RI process loads on brain regions placed bilaterally in the prefrontal and parietal lobe, the generation of new solutions mostly relies on activity of subcortical, temporal and occipital cortex regions. Qualitatively, a more left-lateralized activation for RI processes seem to be present, mostly related to inferior and middle frontal gyrus activation, as well as activation in the precuneus. Differently, subcortical activations are more pronounced during RA steps, with the thalamus and the caudate nuclei playing a major role. These results have been confirmed by a statistical comparison of the two maps through permutation-based statistics, also highlighting a very small area of overlap located in the superior/medial frontal lobe (see Fig. 6 and Table 7).

3.1.4. Gf and resting-state brain functional networks

Results for the overlap with ALE G*f* maps are reported in Fig. 7. In general, RSN maps showed a significant amount of overlap with each G*f* map, with exception of RA map, possibly due to its highly-fragmented nature. The overlap for G*f* ALE maps was as follows: G*f* = 56.8%; vG*f* = 83.2%; vsG*f* = 80.3%; higher complexity = 61.7%; rule inference = 42.3%; rule application = 31.5% (Fig. 7).

The analysis revealed a clear overlap between G*f* and several RSNs, with a pivotal role played by regions of the AN. For both global G*f*, vG*f* and vsG*f* maps, the overlap with regions of the AN was at least double that of other networks, with the AS, BG and LECN networks as second major contributors. Interestingly, facing more difficult trials seems to require the additional activation of regions of the LECN and Language networks. Finally, RI processing still requires AN activity and a second major contribution by the AS, while engaging in producing new solutions seems to engage a multi-network substrate encompassing the RECN, Auditory, AS, Precuneus, Language and BG, while regions of the AN show little to no overlap. It should be noted that the overlap with RSNs for RA only covers 31.5% of the actual map mostly due to subcortical regions of activation not belonging to any of the RSNs considered for the present analysis.

The overlap between AN and G*f* maps is also visible in Fig. 8A, where a graphical overlay is provided for the RSNs maps by Shirer et al., Yeo et al. and the recent multimodal functional parcellation of the human brain by Glasser et al. A greater overlap is clearly visible for regions of the parietal lobe, while prefrontal G*f* nodes might be associated with both Fronto-parietal and Dorsal Attention networks (Fig. 8B). Detailed considerations about the role of the different RSNs in G*f*-related cognitive processing are included in the Discussion section. A further anatomical mapping of G*f* nodes with respect to a cortico-subcortical lobar brain parcellation is also available in Fig. 9, showing the overlap between each G*f*-ALE map and five lobes (prefrontal, parietal, temporal, occipital, limbic), the cerebellum and the brainstem. Values have been calculated as the ratio between the label assigned to each ALE map cluster (e.g. prefrontal) by the ALE software and the total number of significant clusters in each ALE map. Comments on these results are included as part of the Discussion section.

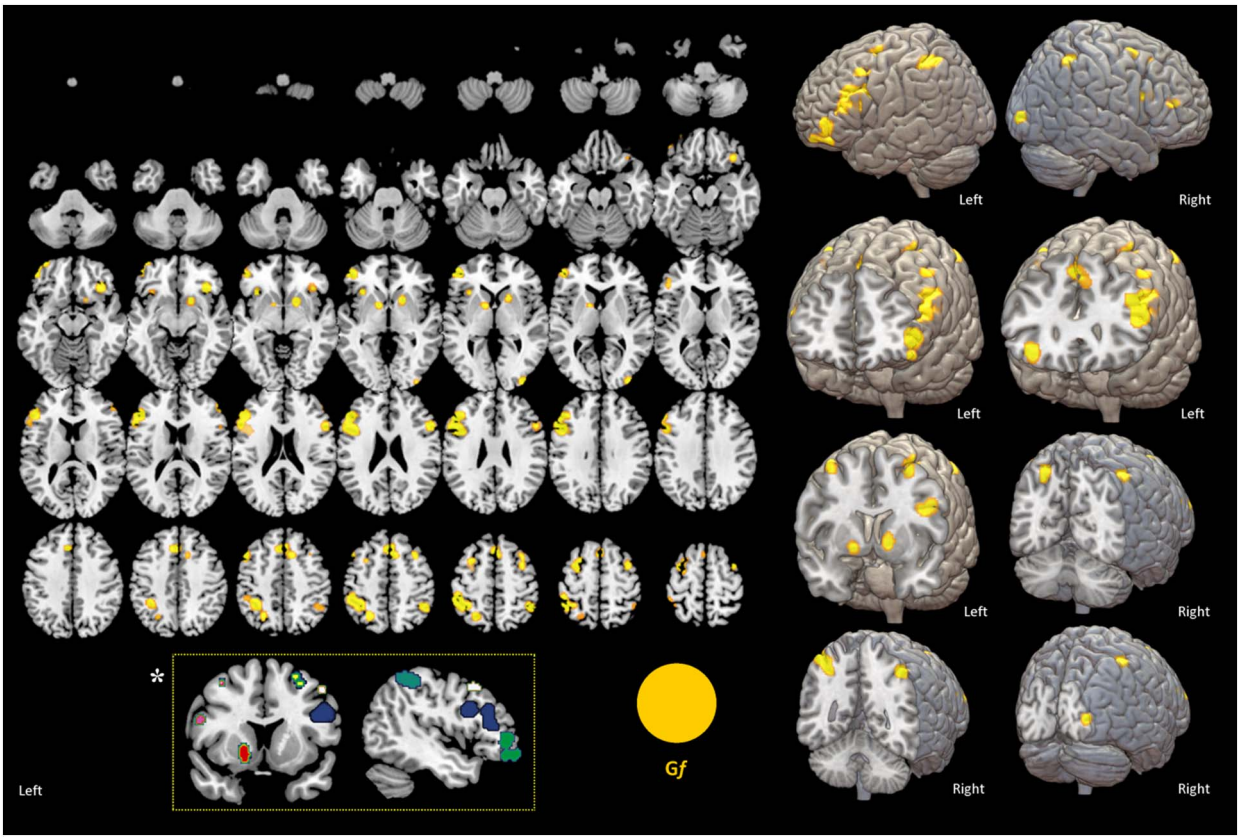

Fig. 1. Fluid intelligence in the human brain. The results of cluster-based statistics performed on the entire dataset of studies are shown. The map refers to studies assessing G*f* by means of visuospatial and verbal tasks, without discriminating by trial or task types. The map is therefore a non-specific, global representation of G*f* processing in the brain. A complete set of coordinates for each cluster is available in Table 1. All the G*f* ALE maps are available at www.tmslab.com/santalab.php. A parcellation of each ALE map in clusters is also provided, as shown in *, where each color represents a segregated functional activation cluster identified by the ALE analysis. (For interpretation of the references to color in this figure legend, the reader is referred to the web version of this article.)

4. Discussion

We derived spatial maps representing the anatomical localization of cognitive processes related to abstract reasoning and problem solving commonly ascribed to G*f*. A classification of available studies on the basis of the type of stimuli used to assess G*f* (verbal and visuospatial), the different problem solving stages (rule inference and rule application) and task difficulty, allowed us to identify spatially segregated networks of cortical and subcortical regions playing a relevant role G*f* processing. Moreover, anatomical mapping suggested an overlap between G*f*-related brain regions and resting-state networks related to attention, salience and cognitive control. The relevance of the different networks identified might provide useful insight for neurostimulation and cognitive training interventions.

4.1. Gf: attention, salience and cognitive control

The anatomical mapping and functional connectivity analyses provided a novel overview of brain correlates of G*f*. Since the first neuroimaging evidence of G*f*-related activations using PET imaging (R.J. Haier et al., 1988), a major role for regions in the prefrontal and parietal lobes of the brain has been suggested and supported by extensive literature (R. Colom et al., 2009). While such fronto-parietal centric view of human intelligence seems a reasonable assumption given the vast array of cognitive functions loading on prefrontal and parietal regions (e.g. attention, memory, language), the exact localization of those regions activated during abstract reasoning suggest the involvement of multiple functional networks potentially responsible for different, non-overlapping components of G*f* processing. During the last two decades, the rise of functional connectivity analysis has stressed the importance of examining brain activity in terms of network dynamics, putting forward the idea of an ongoing, spontaneous coordinated activity built on–if solely canonical neuroanatomy is taken into account–apparently unrelated regions (Achard & Bullmore, 2007; Sporns, 2013). Indeed, the overlap between G*f* and RSN nodes have provided multiple insights: (i) G*f*-related processing is mostly linked to the activity of a fronto-parietal network highly resembling the attention network, (ii) with minor contributions by regions of the anterior salience, left executive control network, right executive control network and basal ganglia network; (iii) activation patterns for verbal and visuospatial stimuli differ for the additional contribution of right executive control network regions required during vsG*f* processing; as discussed in the next paragraph, (iv) more difficult trials requires a significant additional contribution by nodes of the left executive control network; finally, (v) processing stages involving rule inference and rule application clearly differ in terms of their RSNs correlates (see dedicated paragraph).

Overall, the role of the Attention Network constitutes the more striking finding, and suggest the need for discussion about what have been labeled as "fronto-parietal" correlates of G*f* so far. Commonly, the term "fronto-parietal network" refers to a slightly different–or just broader—set of regions including a large number of Brodmann areas: [prefrontal lobes] BA6, 9, 10, 11, 44, 45, 46, 47, 32; [parietal lobes] BA5, 7, 39, 40 (Jung & Haier, 2007). The list of cognitive functions expressed by these regions is extensive, spanning from attention to visuospatial working memory, verbal working memory, short-term memory, mental rotation, language production and comprehension, cognitive control, inhibition and switching (for a review see (Jung & Haier, 2007)). In a prior attempt to define overlapping and dissociable nodes for G*f* and G*c*, Colom and colleagues have stressed out

Table 1
G*f* nodes information. Volume, coordinates and corresponding Brodmann area, lobe, hemisphere and regional labels are reported for each cluster included in the ALE map for G*f*.

Cluster number	Volume (mm^3)	Weighted center			Extrema value	Extrema value coordinates			Brodmann area	Hemisphere	Lobe	Label
		x	*y*	*z*		*x*	*y*	*z*				
G*f*												
1	7432	− 49.74	21.1	24.87	0.040	− 50	12	30	9	L	Frontal	Inferior frontal gyrus
					0.030	− 48	30	16	46	L	Frontal	Middle frontal gyrus
					0.020	− 54	28	32	9	L	Frontal	Middle frontal gyrus
					0.020	− 56	20	18	9	L	Frontal	Inferior frontal gyrus
2	4424	− 41.96	− 44.05	52.4	0.030	− 46	− 42	56	40	L	Parietal	Inferior parietal lobule
					0.027	− 36	− 44	46	40	L	Parietal	Inferior parietal lobule
3	3360	− 45.45	49.71	− 7.25	0.028	− 46	46	2	46	L	Frontal	Inferior frontal gyrus
					0.022	− 46	54	− 14	10	L	Frontal	Middle Frontal Gyrus
					0.021	− 36	58	− 16	10	L	Frontal	Middle frontal gyrus
					0.019	− 48	46	− 14	10	L	Frontal	Inferior frontal gyrus
4	2840	0.43	22.44	48.81	0.022	− 4	24	46	6	L	Frontal	Medial frontal gyrus
					0.018	6	18	50	6	R	Frontal	Superior frontal gyrus
					0.018	10	16	48	32	R	Frontal	Medial frontal gyrus
5	1448	− 30.55	4.05	59.37	0.017	− 30	10	54	6	L	Frontal	Middle frontal gyrus
					0.017	− 32	2	60	6	L	Frontal	Middle frontal gyrus
					0.016	− 34	0	66	6	L	Frontal	Middle frontal gyrus
					0.016	− 26	12	58	6	L	Frontal	Middle frontal gyrus
6	1088	35.64	27.94	− 12.07	0.033	36	28	− 12	47	R	Frontal	Inferior frontal gyrus
7	968	16.52	11.26	− 4.82	0.022	16	10	− 6		R	Sub-cortical	Putamen
8	944	− 24.91	− 61.21	50.77	0.023	− 24	− 62	52	7	L	Parietal	Superior parietal lobule
9	896	45.21	− 49.32	52	0.026	46	− 50	52	40	R	Parietal	Inferior parietal lobule
10	864	34.61	8.18	55.57	0.019	34	4	56	6	R	Frontal	Middle frontal gyrus
					0.017	34	16	52	6	R	Frontal	Middle frontal gyrus
11	808	52.92	16.48	23.3	0.026	52	16	24	9	R	Frontal	Inferior frontal gyrus
12	592	− 48.41	16.94	48.16	0.021	− 50	20	48	6	L	Frontal	Middle frontal gyrus
13	584	52.86	40.21	18.76	0.020	54	38	20	46	R	Frontal	Middle frontal gyrus
					0.017	50	48	22	46	R	Frontal	Middle frontal gyrus
14	528	35.59	− 91.87	2.75	0.023	36	− 92	4	18	R	Occipital	Middle occipital gyrus
15	488	− 13.22	5.12	− 0.31	0.018	− 12	4	0		L	Sub-cortical	Globus pallidus
16	392	− 33.79	22.14	− 3.89	0.018	− 34	22	− 6		L	Sub-cortical	Insula

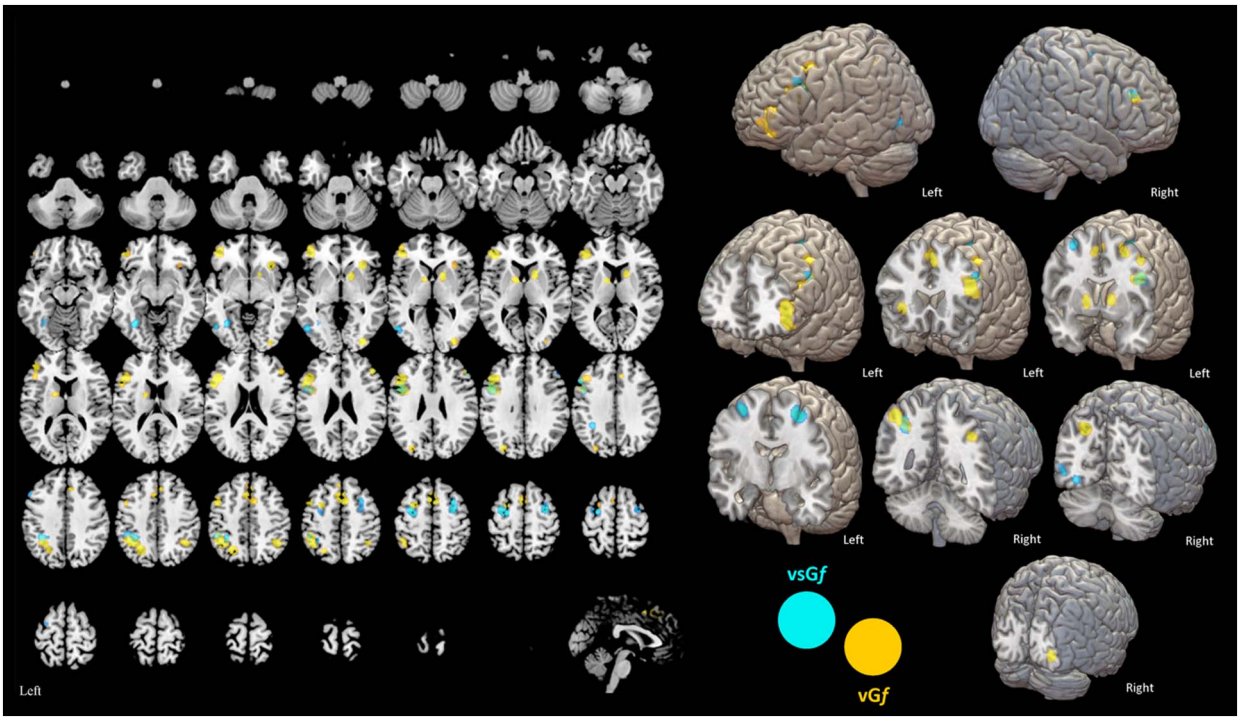

Fig. 2. Average activation during more challenging trials. Areas of activation during most difficult trials (both visuospatial and verbal, yellow) respect to those consistently activated during all trials (blue). A more localized activation of regions placed in the bilateral prefrontal lobe, anterior cingulate cortex and bilateral temporo-occipital junction is visible (green areas shows overlap between the two maps). A complete set of coordinates for each cluster is available in Table 2. (For interpretation of the references to colour in this figure legend, the reader is referred to the web version of this article.)

Table 2
Activation pattern for more complex trials. Volume, coordinates and corresponding Brodmann area, lobe, hemisphere and regional labels are reported for each cluster included in the ALE map summarizing activation foci recorded for more difficult trials, regardless of the nature of the stimuli (verbal, visuospatial).

Cluster number	Volume (mm^3)	Weighted center			Extrema value	Extrema value coordinates			Brodmann area	Hemisphere	Lobe	Label
		x	*y*	*z*		*x*	*y*	*z*				
Complexity												
1	2832	77	65	59	0.020	− 40	60	− 10	10	L	Frontal	Middle frontal gyrus
					0.010	− 48	48	− 20	11	L	Frontal	Middle frontal gyrus
					0.095	− 50	42	− 18	47	L	Frontal	Inferior frontal gyrus
2	1976	5	7	11	0.018	− 48	8	26	9	L	Frontal	Inferior frontal gyrus
					0.014	− 40	12	36	9	L	Frontal	Precentral gyrus
3	1376	11	44	52	0.020	− 34	16	54	6	L	Frontal	Middle frontal gyrus
					0.009	− 42	18	46	6	L	Frontal	Middle frontal gyrus
4	1160	98	53	8	0.002	30	22	38	8	R	Frontal	Middle frontal gyrus
					0.001	34	20	32	8	R	Frontal	Middle frontal gyrus
5	840	27	15	5	0.014	− 14	6	− 4		L	Sub-cortical	Lentiform nucleus
6	832	87	9	88	0.017	− 34	− 46	48	40	L	Parietal	Inferior parietal lobule
					0.008	− 44	− 52	50	40	L	Parietal	Inferior parietal lobule
7	760	3	42	21	0.000	10	34	32	6	R	Frontal	Medial frontal gyrus
					0.010	0	40	30	9	L	Frontal	Medial frontal gyrus
8	560	83	4	94	0.013	14	10	− 6	.	R	Sub-cortical	Caudate
					0.009	20	14	0	.	R	Sub-cortical	Lentiform nucleus
9	552	43	35	> 98	0.010	− 28	− 64	56	7	L	Parietal	Superior parietal lobule
					0.010	− 40	− 66	56	7	L	Parietal	Inferior parietal lobule
10	520	26	4	39	0.016	54	14	24	9	R	Frontal	Inferior frontal gyrus
11	512	41	24	2	0.016	12	20	48	6	R	Frontal	Superior frontal gyrus
12	496	3	71	73	0.015	− 18	− 4	14	.	L	Sub-cortical	Thalamus
13	488	39	95	34	0.015	36	− 68	42	19	R	Parietal	Precuneus
14	480	5	63	26	0.015	60	− 46	10	21	R	Temporal	Middle temporal gyrus
15	464	6	83	1	0.015	− 60	− 54	12	22	L	Temporal	Superior temporal gyrus
16	400	62	83	87	0.001	46	34	− 2	13	R	Frontal	Inferior frontal gyrus
17	376	37	6	93	0.013	36	28	− 10	47	R	Frontal	Inferior frontal gyrus
18	352	74	52	37	0.015	40	− 70	52	7	R	Parietal	Superior parietal lobule

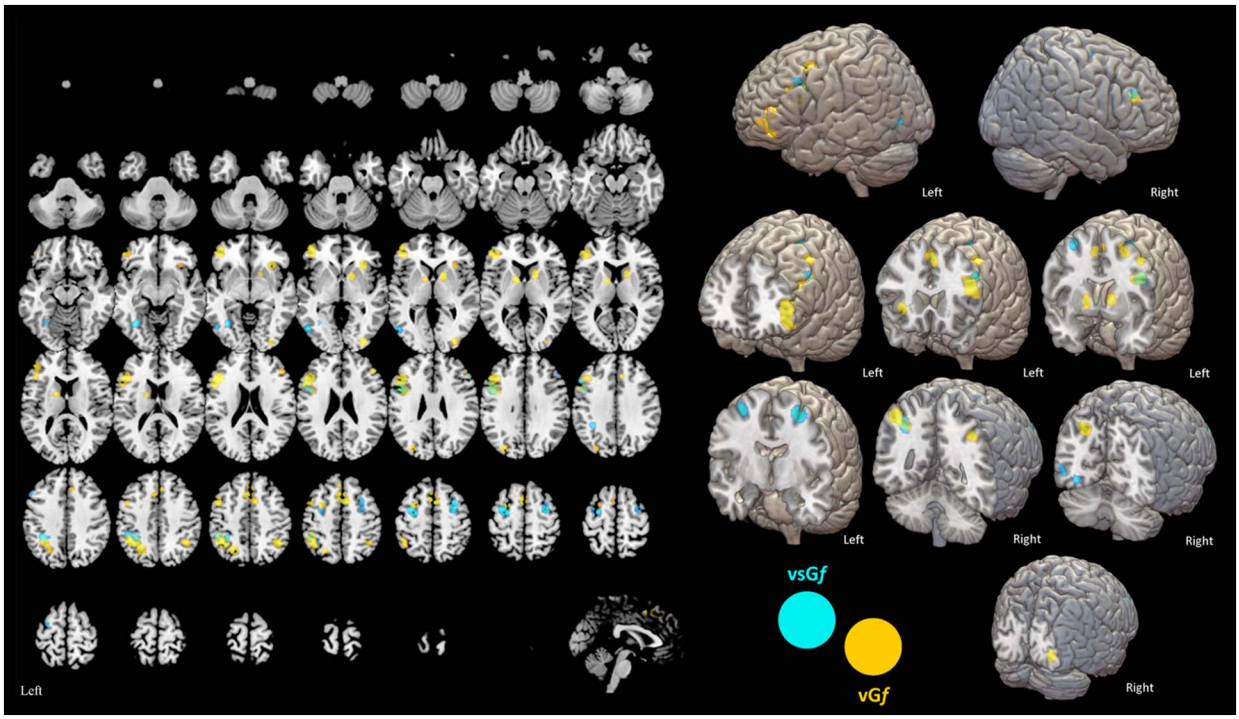

Fig. 3. Average activation during verbal and visuospatial processing. Areas of activation during verbal and visuospatial tasks are respectively highlighted in yellow and blue. A complete set of coordinates for each cluster is available in Table 3. This map only show a quantitative estimate of activation for each modality and a simple qualitative overlap of the two maps. A permutation-based statistical comparison of the two modalities is reported in Fig. 4. (For interpretation of the references to colour in this figure legend, the reader is referred to the web version of this article.)

specific roles for such regions even more, including anatomical correlates for specific subprocesses such as symbolism, abstraction, hypothesis testing and response selection, providing an comprehensive map including almost the entire prefrontal and parietal lobes (R. Colom et al., 2009).

Notably, these regions overlap with three or more RSNs, namely the dorsal and ventral attention networks (as conceptualized by Corbetta et al.), the default mode network (Raichle, 2015), the fronto-parietal control network (by Dosenbach et al., labeled executive control network in the present work) and the cingulo-opercular network (by Dosenbach et al., labeled anterior salience in the present work). This might lead to misleading interpretation of results across studies and a missed opportunity to look at G*f* correlates at the network level in a meaningful way. Our analysis suggests a tighter link between G*f* and attention network's activity in humans, arguing for a shift in the conventional definition of the fronto-parietal correlates of high-order cognition, usually associated with the activity of regions involved in cognitive control, i.e. the left-right executive control networks. Though, at a more theoretical level, it must be noted that this does not mean individual G*f* abilities are more tightly associated with attention per se. Several behavioral evidences have disentangled the interplay between G*f*, attention and executive functions, actually showing moderate associations (for a review see (Colom et al., 2016b)). For instance, a very small portion of G*f* variance was explained by attention control in the study by Unsworth and Spillers (Unsworth, Spillers, & Brewer, 2010), while Chuderski et al. have shown that inhibition, interference resolution, and attention control are not related to G*f* once short-term storage capacity is controlled for (Chuderski & Necka, 2012). Even though these evidences do not diminish the intriguing overlap with attention-related regions highlighted in the present analysis, ad-hoc combined resting-state/evoked fMRI studies are needed to fully understand the role of attention-network regions in G*f* processing.

It should also be noted that a discrepancy between the Shirer et al. RSNs parcellation and the one proposed by another group (i.e. Yeo et al., 2011) is present and visible in Fig. 8(A): G*f* nodes in the prefrontal lobe are primarily labeled as part of the fronto-parietal control network in the work by Yeo et al., while Shirer and colleagues show a bigger prefrontal AN component covering the vast majority of G*f* nodes. Clearly, a definitive parcellation in RSNs is not available and different analytical approaches might yield to slightly different labels; however, by considering how (i) Yeo et al. parcellation also associates G*f* with prefrontal nodes of the AN, and that (ii) the attention network in the parietal lobes show full overlap with G*f* in both parcellations (see Fig. 8B), we consider our conclusion of a major role for the AN in explaining G*f*-related activations still pertinent.

Activity within the Anterior Salience network (cingulo-opercular in Dosenbach et al.) is also relevant, possibly for stable maintenance of task and rule mode (Bunge et al., 2005) as well as performance monitoring (M. M. Botvinick et al., 2004; M. M. Botvinick, Braver, Barch, Carter, & Cohen, 2001; Carter et al., 1998). Finally, the activity in the executive control network (FPCN in Dosenbach et al.) is also relevant but to a lesser extent, for control over attention allocation and to provide flexibility by adjusting response to feedback. Notably, all these activation layers show a dominant left-sided activation, regardless of stimulus type (verbal and visuospatial).

We here suggest a more relevant role for the dorsal and ventral portion of the AN as in G*f* related cognitive processing. Following the definition by Corbetta and colleagues (Corbetta et al., 2008), the attention network is composed by a dorsal fronto-parietal (or dorsal attention) component, which enable the selection of sensory stimuli based on internal goals or expectations (i.e. goal-driven attention) and links them to appropriate motor/cognitive responses; and a ventral fronto-parietal (or ventral attention) component, detecting salient and behaviorally relevant stimuli in the environment, especially when unattended (stimulus-driven attention). These definitions has been also corroborated by experimental work using transcranial magnetic stimulation (TMS) to causally induce a modulation of dorsal parietal lobe activity, with effects over visuospatial attention in humans (Thut, Nietzel, & Pascual-Leone, 2005). A relevant role for attention while solving an abstract reasoning task is intuitively reasonable, however

Table 3
Visuospatial and Verbal G*f* activation foci. Volume, coordinates and corresponding Brodmann area, lobe, hemisphere and regional labels are reported for each cluster included in G*f* maps obtained from studies testing vsG*f* and vG*f*.

Cluster number	Volume (mm^3)	Weighted center			Extrema value	Extrema value coordinates			Brodmann area	Hemisphere	Lobe	Label
		x	*y*	*z*		*x*	*y*	*z*				
vsG*f*												
1	1704	− 48.45	9.39	29.97	0.018	− 48	8	30	9	L	Frontal	Inferior frontal gyrus
					0.011	− 52	20	36	9	L	Frontal	Middle frontal gyrus
2	1360	− 30.53	− 5.83	57.18	0.018	− 30	− 6	56	6	L	Frontal	Precentral gyrus
3	1088	29.95	0.63	55.1	0.016	30	− 2	56	6	R	Frontal	Middle frontal gyrus
					0.011	30	10	52	6	R	Frontal	Middle frontal gyrus
4	920	− 34.72	− 44.87	41.65	0.016	− 36	− 44	40	40	L	Parietal	Inferior parietal lobule
5	520	− 33.42	− 60.86	− 8.83	0.013	− 34	− 62	− 8		L	Cerebellum	Declive
6	440	− 46.38	− 40.46	46.72	0.011	− 48	− 40	46	40	L	Parietal	Inferior parietal lobule
7	432	− 50.06	− 68.29	− 1.63	0.012	− 50	− 68	− 2	1	L	Temporal	Inferior temporal gyrus
8	320	51.22	33.2	28.63	0.014	52	34	28	9	R	Frontal	Middle frontal gyrus
vG*f*												
1	8200	− 46.37	25.62	18.03	0.031	− 46	24	22	46	L	Frontal	Middle frontal gyrus
					0.028	− 46	8	30	9	L	Frontal	Inferior frontal gyrus
					0.026	− 44	40	6	46	L	Frontal	Inferior frontal gyrus
					0.022	− 52	16	20	44	L	Frontal	Inferior frontal gyrus
					0.020	− 44	42	− 4	46	L	Frontal	Inferior frontal gyrus
2	3984	− 36.31	− 52.96	45.97	0.027	− 44	− 46	48	40	L	Parietal	Inferior parietal lobule
					0.024	− 24	− 64	46	7	L	Parietal	Precuneus
					0.021	− 38	− 52	44	40	L	Parietal	Inferior parietal lobule
3	2648	− 0.01	15.37	50.46	0.020	2	10	52	6	L	Frontal	Superior frontal gyrus
					0.019	− 2	10	56	6	L	Frontal	Medial frontal gyrus
					0.015	8	28	38	32	R	Limbic	Cingulate gyrus
					0.013	− 2	32	48	8	L	Frontal	Superior frontal gyrus
					0.013	0	30	44	8	L	Frontal	Medial frontal gyrus
4	1032	14.91	9.66	2.28	0.020	16	10	4		R	Sub-cortical	Caudate
5	736	40.19	− 52.15	45.83	0.021	42	− 54	46	40	R	Parietal	Inferior parietal lobule
6	720	− 13.83	1.99	8.35	0.017	− 12	2	6		L	Sub-cortical	Lentiform nucleus
					0.015	− 18	0	16		L	Sub-cortical	Caudate
7	680	31.83	24.67	− 3.67	0.025	32	24	− 4		R	Sub-cortical	Claustrum
8	592	31.24	− 87.92	− 1.26	0.023	32	− 88	0	18	R	Occipital	Middle occipital gyrus
9	552	− 46.67	8.18	47.87	0.019	− 46	8	48	6	L	Frontal	Middle frontal gyrus
10	512	− 27.66	3.61	54.43	0.017	− 28	4	52	6	L	Frontal	Middle frontal gyrus
					0.017	− 26	4	56	6	L	Frontal	Middle frontal gyrus
11	400	47.8	33.33	23.75	0.016	46	34	22	9	R	Frontal	Middle frontal gyrus
12	400	− 30.68	− 78.82	30.92	0.020	− 30	− 78	32	19	L	Occipital	Superior occipital gyrus

our data shows attention-related regions as constituting a pivotal shared substrate of one's cognitive effort during G*f* testing. A conclusion would be that individual differences in G*f* are more related to the ability to focus on the task at hand while also suppressing distractors (both endogenous and exogenous), therefore maximizing cognitive capacity over relevant information. The competition model of attention proposes that objects in a visual scene compete for access to visual short-term memory and that the competition is biased by top-down signals that promote access of behaviorally relevant objects (Desimone & Duncan, 1995). These top-down signals, characterized as working memory (Downing, 2000), long-term memory (Moore & Armstrong, 2003), or action-related (Craighero, Bello, Fadiga, & Rizzolatti, 2002), interact with sensory (bottom-up) signals produced by objects in the visual scene, enabling the desired object to be selectively perceived/encoded and get access to memory storage at the expense of unimportant objects (Bundesen, 1990). Reducing the amount of information to be stored at any given moment could create significant cascade effects over higher order processes related to G*f*, e.g. hypothesis testing and validation. If only relevant information enters working memory, more hypotheses can be tested, with a consequent dramatic advantage for cognitive abilities tested using time-constrained assessment. Pushing the argument a bit further, evidence of increased activity in sensory regions (i.e. visual cortex) in subjects with high-functioning autism has been documented as the only significant correlates of their above-average G*f* abilities (Soulieres et al. 2009), with trial complexity-related allocation of resources still characterized by increased occipito-temporal activity (Simard, Luck, Mottron, Zeffiro, & Soulieres, 2015). An advantage in attention allocation might be relevant as much as a more effective encoding of visual stimuli during the very first stage of processing, suggesting higher G*f* abilities might be more related to

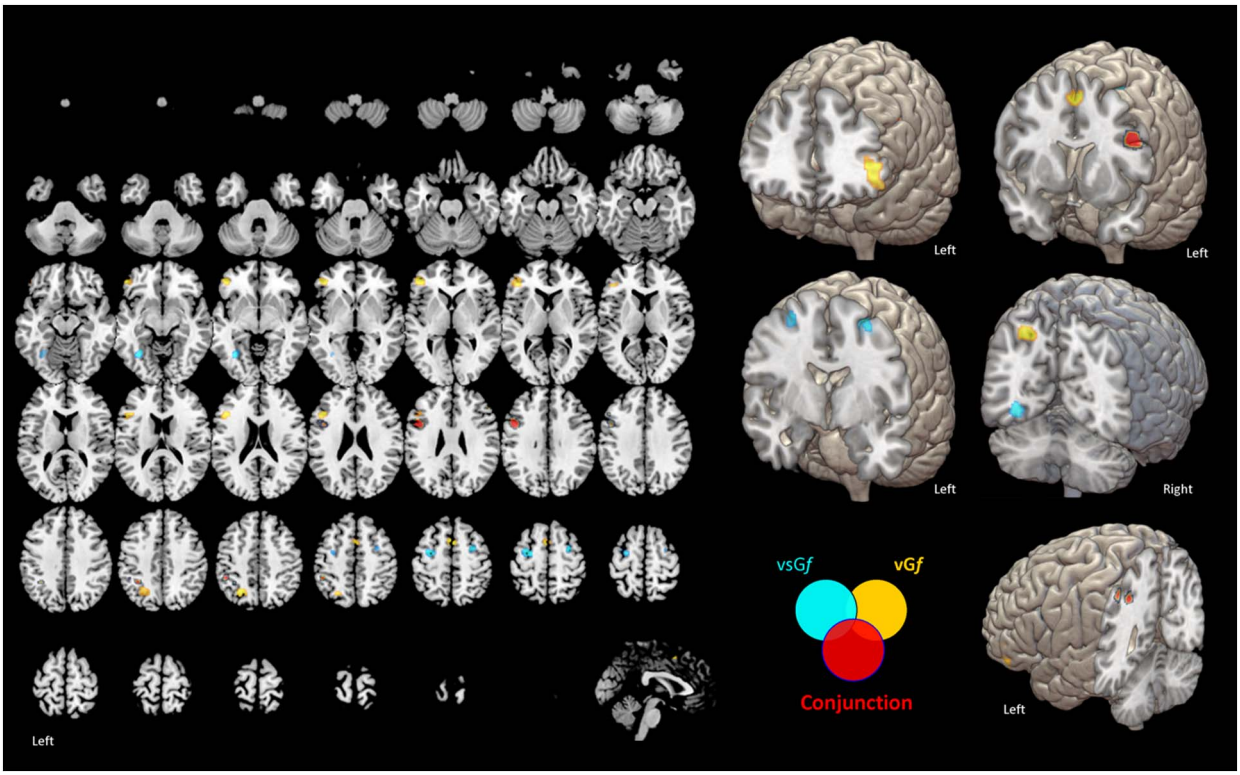

Fig. 4. Statistical comparison of vG*f* and vsG*f* activations. A permutation-based statistical comparison has been implemented to highlight regions exclusively belonging to each of the two trial types, as well regions significantly activated during both trials. Regions of overlap are localized in the left prefrontal and parietal lobes, more specifically in the inferior frontal lobe (BA9) and inferior parietal lobe (BA40). A complete set of coordinates for each cluster is available in Table 4. Note: BA = Brodmann area.

Table 4
Modality-specific and overlapping foci. Volume, coordinates and corresponding Brodmann area, lobe, hemisphere and regional labels are reported for each cluster exclusively included in the ALE map of vG*f* studies, vsG*f* studies or both.

Cluster number	Volume (mm^3)	Weighted center			Extrema value	Extrema value coordinates			Brodmann area	Hemisphere	Lobe	Label
		x	*y*	*z*		*x*	*y*	*z*				
Verbal G*f* > visuospatial G*f*												
1	1184	− 45.49	40.76	− 0.85	3.090	− 47	40	0	46	L	Frontal	Inferior frontal gyrus
					2.512	− 44	40	− 4	46	L	Frontal	Inferior frontal gyrus
					2.366	v	36	4	46	L	Frontal	Inferior frontal gyrus
					2.144	− 50	40	− 8.67	47	L	Frontal	Middle frontal gyrus
					1.812	− 49	44	− 10	46	L	Frontal	Inferior frontal gyrus
					1.717	− 44	36.25	8.75	46	L	Frontal	Inferior frontal gyrus
2	592	− 46.66	20.69	21.04	2.170	− 42	20	20	46	L	Frontal	Middle frontal gyrus
					1.960	− 52	18	20	9	L	Frontal	Inferior frontal gyrus
3	576	− 25.09	− 61.58	46.05	2.226	− 28	− 60	48	7	L	Parietal	Superior parietal lobule
					1.896	− 22	− 62	44	7	L	Parietal	Precuneus
4	456	− 1.29	8.43	54.22	2.748	− 4	6	54	6	L	Frontal	Medial frontal gyrus
Visuospatial G*f* > Verbal G*f*												
1	752	− 30	− 6.29	56.7	2.878	− 29	− 6	57	6	L	Frontal	Precentral gyrus
2	456	− 33.02	− 60.23	− 8.7	2.326	− 32.37	− 59.37	− 8.06		L	Cerebellum	Declive
3	272	28.44	− 0.61	55.24	2.034	28	1	57	6	R	Frontal	Sub-gyral
Verbal G*f* AND visuospatial G*f*												
1	1248	− 47.61	8.45	29.53	0.018	− 48	8	30	9	L	Frontal	Inferior frontal gyrus
2	248	− 46.48	− 41.42	48.09	0.011	− 48	− 40	46	40	L	Parietal	Inferior parietal lobule
3	160	− 34.98	− 47.02	42.15	0.014	− 36	− 46	42	40	L	Parietal	Inferior parietal lobule
4	64	51	31.59	27.05	0.013	52	32	28	9	R	Frontal	Middle frontal gyrus
5	32	− 50.51	21.5	34.5	0.009	− 52	22	34	9	L	Frontal	Middle frontal gyrus
6	16	− 34.95	− 50	48	0.009	− 34	− 50	48	40	L	Parietal	Inferior parietal lobule

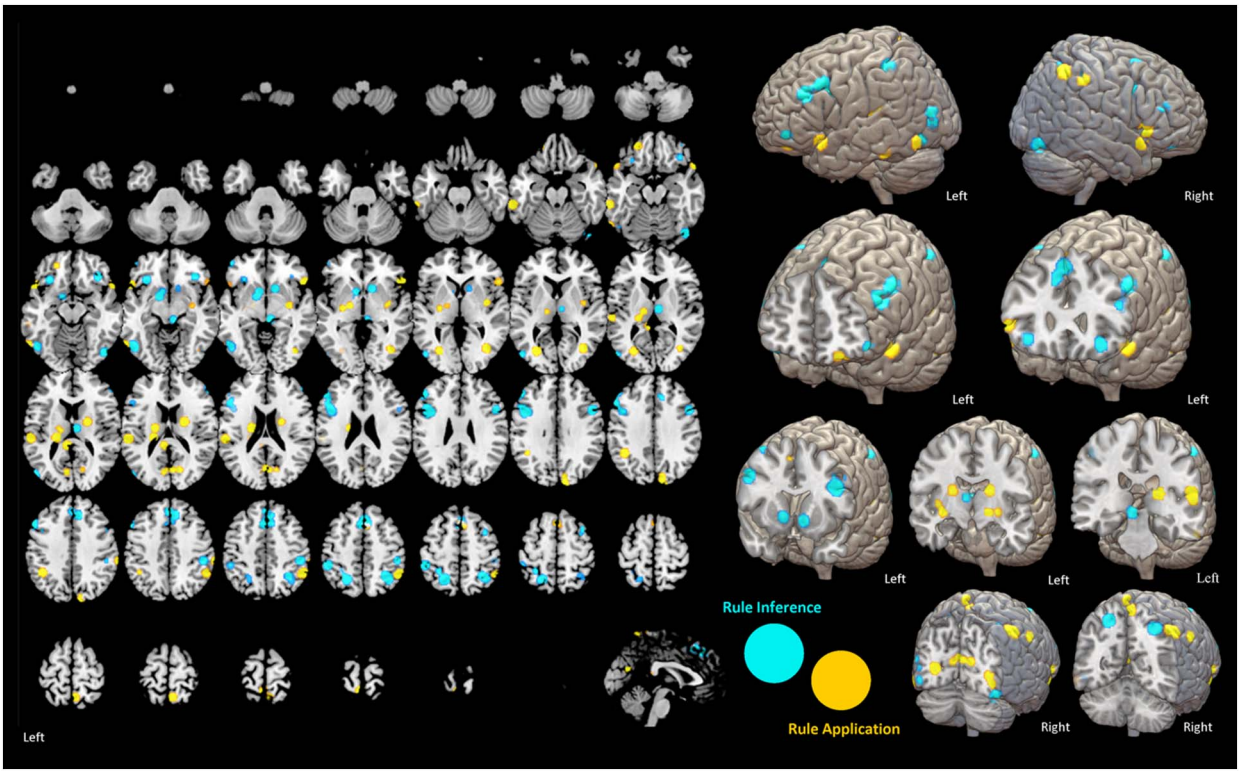

Fig. 5. Brain activity during rule inference and rule application processing stages. Two maps are shown, referring to the average fMRI activation identified during trials requiring to understand the logical or relational rule governing the stimuli being administered (blue), as well as during the application of a previously identified rule on new stimuli (yellow). A complete set of coordinates for each cluster is available in Tables 5 and 6. These maps only show a quantitative estimate of activation for each processing step and a simple qualitative overlap of the two maps. A permutation-based statistical comparison of the two trial modalities is reported in Fig. 7. (For interpretation of the references to colour in this figure legend, the reader is referred to the web version of this article.)

optimization of low-level cognitive processes (visual, auditory, somatomotor) and their top-down control by attentional systems, then pure computational power related to the final stages of processing. Interestingly, the relevance of attention network structures for human cognition also assume an evolutionary perspective: a comparison of attention network, specifically its dorsal component, in the human and macaque brains have recently highlighted significant differences in its extension and functional role, with the authors concluding that "…*results suggest that the human and macaque attention systems have evolved in the service of the unique challenges facing each species, and in humans this has meant an elaboration of the attention control system to support new and unique functions that may underlie expanded social cognition abilities*" (Patel et al., 2015). The present findings do not diminish the specific role of regions related to hypothesis testing or manipulation of logical operators, though suggest that being smarter might primarily mean being more efficient in allocating resources, a property as important as being able of performing complex logical operations (Richard J. Haier, Siegel, Tang, Abel, & Buchsbaum, 1992).

While no studies have investigated the role of the Attention Network as a neurobiological substrate for G*f*-related capacity, a recent study has proposed a major role for the salience network (Yuan et al., 2012). The pivotal node of the anterior salience network, i.e. dACC and anterior insula, have been extensively associated with cognitive control and error detection in humans given their involvement in top–down control over sensory (Crottaz-Herbette & Menon, 2006) and limbic brain regions (Etkin, Egner, Peraza, Kandel, & Hirsch, 2006). While these functions might be relevant for the solution of a G*f* task, other authors also stress the link between these regions and arousal-related processes (Braver & Barch, 2006). Studies by Dosenbach and colleagues show these regions as mostly associated with task-initiation cues and error cues, a potential proof of their role in both control/monitoring and—more simplistically—arousal (given the relevance of the cues) which is then also maintained at an above-baseline level throughout the duration of the task (Dosenbach et al., 2008, 2006).

Overall, the present results stress a major contribution by attention-related regions during G*f* processing. Specific studies are needed to disentangle the contribution of the different cognitive layers coming into play before, after or simultaneously to the attention network (e.g. visual processing, cognitive control, hypothesis testing and validation, task set maintenance), also including the contribution of specific executive functions such as WM, inhibition and switching (as described in the model by Miyake et al. (Miyake & Friedman, 2012; Miyake et al., 2000): functional connectivity analysis of the interplay of different RSNs, G*f* and executive function nodes might help elucidate the link between working memory and G*f* (Au et al., 2014), potentially suggesting the attention network as a bridge between the two constructs as recently shown in the context of cognitive transfer (Greenwood & Parasuraman, 2016).

4.1.1. *Gf as a diffuse network*

While a distinction between a more logical and a creative brain–arguing for a dominant representation of the two constructs respectively in the left and right brain hemispheres—has been proposed over the last few decades, recent evidence exploring the neural basis of creativity and general intelligence do not support such view (Sprugnoli et al., 2017)(Dietrich & Kanso, 2010)(Lindell, 2011). Our data support the same criticism about the duality of human cognition and hemispheric activity, showing a widespread network responsible for G*f*-related brain processing in humans, with a significantly greater degree of left-lateralization only visible for activation foci in the inferior and middle frontal gyrus. This is in line with the P-FIT model of intelligence proposed by Jung and Haier (Jung & Haier, 2007), where a core set of regions in the bilateral prefrontal and parietal lobes play a pivotal role when IQ-related tasks are performed, with additional contributions by

Table 5
Rule inference. Volume, coordinates and corresponding Brodmann area, lobe, hemisphere and regional labels are reported for each activation cluster of the ALE map summarizing studies where rule inference processes were investigated.

Cluster number	Volume (mm^3)	Weighted center			Extrema value	Extrema value coordinates			Brodmann area	Hemisphere	Lobe	Label
		x	*y*	*z*		*x*	*y*	*z*				
Rule Inference												
1	5048	− 48.69	18.72	30.09	0.029	− 52	34	28	9	L	Frontal	Middle frontal gyrus
					0.027	− 44	10	28	9	L	Frontal	Inferior frontal gyrus
					0.023	− 54	18	40	8	L	Frontal	Middle frontal gyrus
					0.013	− 52	20	20	9	L	Frontal	Inferior frontal gyrus
2	3688	2.52	26.72	45.88	0.024	2	26	48	8	L	Frontal	Superior frontal gyrus
					0.023	8	32	42	8	R	Frontal	Medial frontal gyrus
					0.022	0	36	44	8	L	Frontal	Superior frontal gyrus
					0.016	− 4	18	48	6	L	Frontal	Superior frontal gyrus
3	2032	− 23.22	− 56.57	54.06	0.029	− 22	− 58	54	7	L	Parietal	Superior parietal lobule
					0.015	− 30	− 46	56	7	L	Parietal	Precuneus
4	1712	32.51	− 55.03	51.15	0.026	30	− 54	52	7	R	Parietal	Superior parietal lobule
5	1344	− 11.98	6.54	− 7.39	0.022	− 10	10	− 6		L	Sub-cortical	Caudate
					0.021	− 14	4	− 10		L	Sub-cortical	Lentiform nucleus
6	1120	44.02	− 74.33	− 16.78	0.025	44	− 74	− 16		R	Cerebellum	Declive
7	1112	− 49.08	− 65.81	− 9.99	0.024	− 48	− 66	− 10	37	L	Temporal	Fusiform gyrus
8	1088	48.74	11.28	31.72	0.027	48	12	32	9	R	Frontal	Precentral gyrus
9	1040	− 49.19	− 38.63	52.21	0.027	− 50	− 38	52	40	L	Parietal	Inferior parietal lobule
10	984	47.19	− 32.11	46.17	0.024	48	− 32	46	40	R	Parietal	Inferior parietal lobule
11	768	− 50.41	− 76.68	9.52	0.015	− 52	− 76	12	39	L	Temporal	Middle temporal gyrus
					0.014	− 48	− 76	4		L	Occipital	Inferior temporal gyrus
12	680	− 31.55	26.42	− 11.12	0.022	− 32	26	− 12	47	L	Frontal	Inferior frontal gyrus
13	680	5.53	− 28.6	− 6.23	0.022	6	− 28	− 6		R	Brainstem	
14	672	11.91	14.24	− 3.99	0.022	12	14	− 4		R	Sub-cortical	Caudate
15	67	5.81	− 14.16	10.12	0.022	6	− 14	10		R	Sub-cortical	Thalamus
16	656	35.45	30.98	− 12.73	0.021	36	30	− 12	47	R	Frontal	Inferior frontal gyrus
17	656	− 50.56	49.92	− 8.49	0.022	− 50	50	− 8	46	L	Frontal	Inferior frontal gyrus
18	584	37.36	47.08	− 23.03	0.022	38	48	− 24	11	R	Frontal	Superior frontal gyrus
19	440	53.63	40.49	17.39	0.021	54	40	18	46	R	Frontal	Middle frontal gyrus
20	424	34.63	10.96	58.89	0.019	36	14	62	6	R	Frontal	Middle frontal gyrus
					0.011	34	8	56	6	R	Frontal	Middle frontal gyrus

Table 6
Rule application. Volume, coordinates and corresponding Brodmann area, lobe, hemisphere and regional labels are reported for each activation cluster of the ALE map summarizing studies where rule application processes were investigated.

Cluster number	Volume (mm^3)	Weighted center			Extrema value	Extrema value coordinates			Brodmann area	Hemisphere	Lobe	Label
		x	*y*	*z*		*x*	*y*	*z*				
Rule application												
1	2120	− 20.39	− 19.86	15.65	0.031	− 20	− 14	20		L	Sub-cortical	Caudate
					0.030	− 22	− 26	14		L	Sub-cortical	Thalamus
					0.017	− 14	− 18	8		L	Sub-cortical	Thalamus
2	1920	55.13	22	− 9.3	0.030	58	20	− 16	38	R	Temporal	Superior temporal gyrus
					0.030	52	24	− 4		R	Frontal	Inferior frontal gyrus
					0.015	62	24	− 6	47	R	Frontal	Inferior frontal gyrus
3	1416	50.26	− 50.16	47.95	0.035	50	− 50	48	40	R	Parietal	Inferior parietal lobule
4	1400	− 57.57	− 28	15.38	0.032	− 58	− 28	16	42	L	Temporal	Superior temporal gyrus
5	1160	36.62	− 69.28	2.13	0.031	36	− 68	4	19	R	Occipital	Lingual gyrus
6	1080	2.78	− 71.92	17.31	0.018	4	− 72	18	18	R	Occipital	Cuneus
					0.017	0	− 70	20	31	L	Limbic	Posterior cingulate
					0.017	14	− 72	16	30	R	Occipital	Cuneus
					0.017	− 8	− 76	14	23	L	Occipital	Cuneus
7	1040	10.61	− 87.31	34.9	0.031	10	− 92	36	19	R	Occipital	Cuneus
					0.018	10	− 82	34	19	R	Occipital	Cuneus
8	960	− 29.03	− 72.61	5.26	0.029	− 28	− 72	6		L	Occipital	Lingual gyrus
9	872	− 41.49	− 48.57	36.86	0.030	− 42	− 48	36	40	L	Parietal	Supramarginal gyrus
10	864	20.77	− 5.06	15.81	0.030	20	− 6	16		R	Sub-cortical	Caudate
11	848	− 53.09	19.89	− 12.31	0.030	− 54	20	− 12	47	L	Frontal	Inferior frontal gyrus
12	840	− 7.29	− 37.78	12.71	0.030	− 8	− 38	12		L	Sub-cortical	Thalamus
13	832	− 61.79	− 34.7	− 20.22	0.031	− 62	− 34	− 20	20	L	Temporal	Inferior temporal gyrus
14	776	4.3	− 56.14	68.15	0.031	4	− 56	68	7	R	Parietal	Precuneus
15	680	− 23.59	46.8	− 18.81	0.022	− 24	46	− 20	11	L	Frontal	Middle frontal gyrus
16	680	− 61.09	− 63.5	− 12.92	0.030	− 62	− 64	− 12	37	L	Temporal	Inferior temporal gyrus
17	664	1.75	17.77	54.69	0.018	4	16	52	6	R	Frontal	Superior frontal gyrus
					0.017	0	20	56	6	L	Frontal	Superior frontal gyrus
18	608	− 5.07	− 46.54	75.54	0.030	− 4	− 46	76	7	L	Parietal	Postcentral gyrus
19	584	33.83	− 7.44	− 2.43	0.018	32	− 10	− 6		R	Sub-cortical	Lentiform nucleus
					0.017	36	− 6	2		R	Sub-cortical	Lentiform Nucleus
20	544	− 23.97	− 11.38	− 1.42	0.017	− 30	− 14	0		L	Sub-cortical	Lentiform nucleus
					0.017	− 18	− 10	− 2		L	Sub-cortical	Lentiform nucleus
21	520	63.16	− 32.16	41.64	0.031	64	− 32	42	40	R	Parietal	Inferior parietal lobule

regions of the occipital and temporal lobes supporting both phase-and stimuli-specific processing.

Moreover, the notion of G*f* as a stimulus independent estimate of cognitive processes related to abstract reasoning and problem solving–therefore addressing high order constructs in a "Culture-Fair" manner—does not seem to be fully supported by the available literature, as well as our data. Tasks addressing G*f* by means of language-related stimuli are often reported as showing different patterns of activation respect to visuospatial stimuli (Prado et al., 2010), suggesting that G*f* measurements cannot be a stimulus independent process. The comparison of vsG*f* and vG*f* maps have highlighted how stimuli based on logical reasoning applied to geometrical–i.e. supposedly language unrelated— stimuli (e.g. RAPM, Sandia and Bomat) load on a bilateral network also including temporal and cerebellar structures. These brain areas are not present in the average activation map for language and syntax based G*f* tasks (e.g. A = B, B = C, then A = C), which instead suggests a stronger contribution from subcortical (mostly limbic) structures. Surprisingly, these constitute the major differences between the two processes, with the contribution of parietal and frontal structures showing a balancing between the vG*f* and vsG*f* (20% and 17% for the parietal lobe, and 60% and 54% for the frontal lobe, respectively, Fig. 9). Among these differences, two areas of overlap have been identified, located in the left inferior frontal gyrus and inferior parietal lobe. These regions may constitute a stimulus independent core of G*f* processing as proposed by Krawczyk et al. (Krawczyk et al., 2011), interacting with other cortical and subcortical structures in a stimulus dependent fashion.

Increasing complexity in G*f* trials corresponds to increased activity in multiple regions, including the left inferior frontal lobe, left frontal eye fields, bilateral anterior cingulate cortex and bilateral temporo-occipital junction. Apart from the role played by each specific region, the overlap with RSNs highlights a differential pattern with respect to overall G*f* activation: on top of the activation of attention network regions, more difficult trials require the additional contribution of areas of the left executive control network, which are otherwise not included in any G*f* maps except for a minor contribution during processing of vG*f* stimuli. According to the work by Dosenbach and colleagues (Dosenbach et al., 2006, 2008), the network engaged during more challenging tasks fits with the definition of the (left) fronto-parietal control (FPCN) network. Complementary to the cingulo-opercular/Anterior Salience network, the FPCN is responsible for task engagement, providing flexibility by adjusting control in response to feedback, and is responsible for the online monitoring of cognitive–mostly attentive—resources. For instance, a study by Woldorff et al. showed that regions of the lateral frontal cortex overlapping with the FPCN were active when a cue was interpreted but attention was not shifted (Woldorff et al., 2004), suggesting this network as crucial for increasing the attentive focus while being resilient to "distractors", a potentially

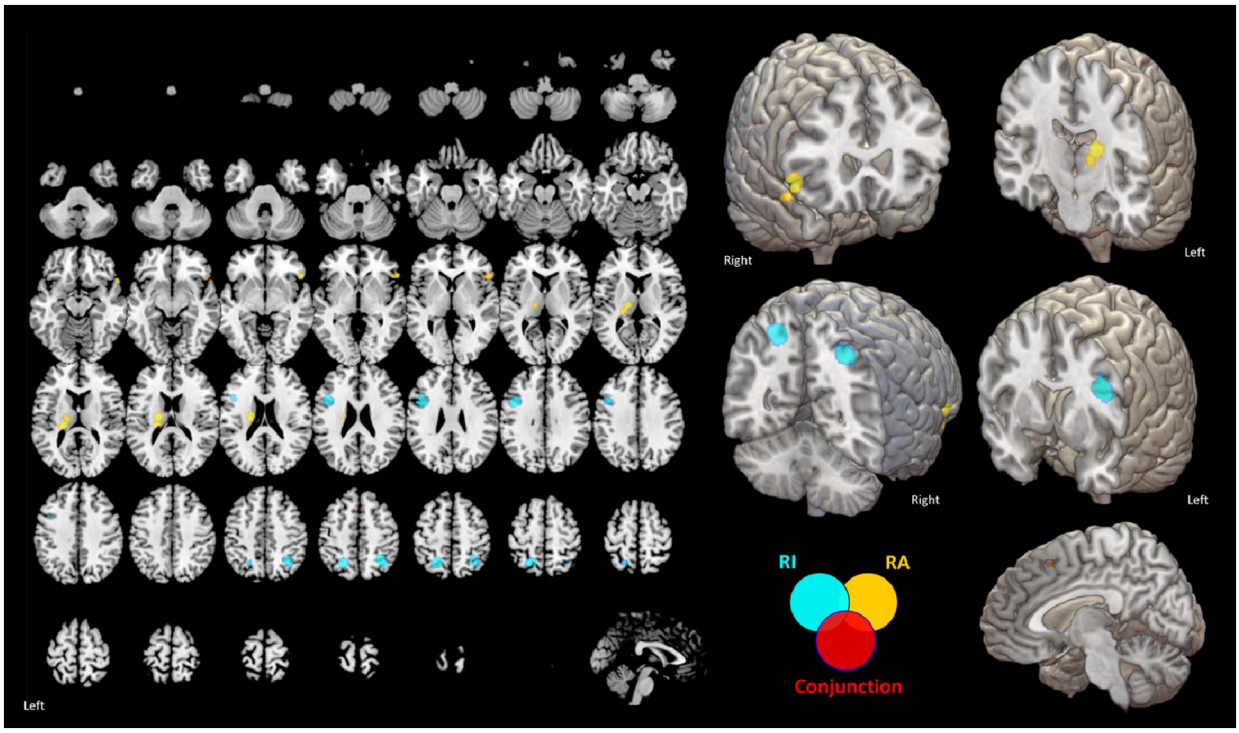

Fig. 6. Statistical comparison of Rule inference and Rule application processing steps. A permutation-based statistical comparison has been implemented to highlight regions exclusively belonging to each of the two processing steps, as well regions significantly activated during both steps. The only region showing a significant (but small in magnitude) degree of overlap is localized in the mesial part of the superior frontal lobe (BA6). A complete set of coordinates for each cluster is available in Table 7. Note: BA = Brodmann area.

crucial function when higher cognitive load trials are faced.

4.1.2. Distinct networks for rule inference and rule application

Solving a G*f* task is a multilevel process including sequential and parallel processing stages referring, for instance, to the understanding of a premise (i.e. the organizational principle behind the stimuli at hand) and the application of previously acquired knowledge to novel stimuli. Our maps highlight the spatial properties of these core processes, regardless of stimulus modality. Results link major differences between rule inference and rule application to a reduced activation of frontal lobe structures as well as an increase of activations in the occipital lobes during rule application. The two processes do not show a significant difference in terms of hemispheric activity, probably showing the more balanced distribution of activation foci in the left and right hemisphere across all the G*f* maps (see Fig. 9). The ALE statistical comparisons show a specific involvement of the thalamus, caudate nuclei and right temporal and frontal lobe structures during rule application, while a dominant role for left-lateralized structures located

Table 7
Rule inference vs rule application. Volume, coordinates and corresponding Brodmann area, lobe, hemisphere and regional labels are reported each cluster exclusively included in the ALE map for RA, RI or both.

Cluster number	Volume (mm^3)	Weighted center			Extrema value	Extrema value coordinates			Brodmann area	Hemisphere	Lobe	Label
		x	*y*	*z*		*x*	*y*	*z*				
Rule application > rule inference												
1	1776	− 19.88	− 18.46	14.91	3.291	− 19.33	− 17.23	14		L	Sub-cortical	Thalamus
					3.090	− 25.83	− 28	13.33		L	Sub-cortical	Thalamus
					2.878	− 17.2	− 13.6	23.2		L	Sub-cortical	Caudate body
2	984	53.63	22.4	− 4.46	3.291	54.1	22.7	− 0.1		R	Frontal	Inferior frontal gyrus
					3.090	53.22	21.71	− 7.27	38	R	Temporal	Superior temporal gyrus
Rule inference > rule application												
1	1912	− 43.77	9.43	28.62	3.291	− 42.8	9.2	28.92	9	L	Frontal	Inferior frontal gyrus
					2.878	− 50	9	27	9	L	Frontal	Inferior frontal gyrus
2	1512	− 21.91	− 58.5	54.21	3.291	− 21.87	− 58.89	54.61	7	L	Parietal	Gray matter
					2.878	− 22	-54	50	7	L	Parietal	Precuneus
3	1344	32.07	− 55.46	50.3	3.291	31.54	− 55.56	50.37	7	R	Parietal	Precuneus
Rule inference and rule application												
1	120	2.47	17.36	51.68	0.013	4	18	50	6	R	Frontal	Superior frontal gyrus
2	8	0	22	54	0.009	0	22	54	6	L	Frontal	Superior frontal gyrus

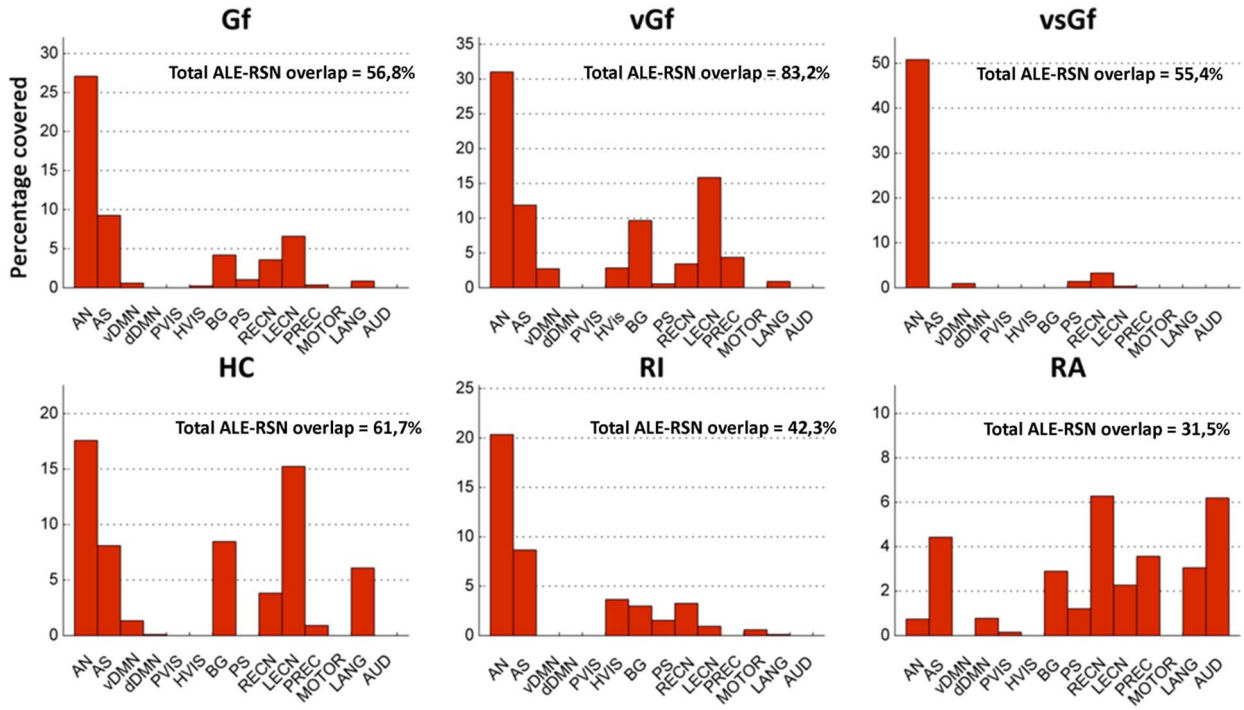

Fig. 7. Anatomical overlap with resting-state fMRI networks. For each significant cluster included in any G*f* map, the percentage of activations occurring in regions belonging to any of the 14 RSNs specified in the method section of the paper is reported. Percentage values refer to the number of voxels composing each ALE map overlapping with each RSN.

in the inferior frontal gyrus and precuneus seems to characterize the Rule Inference process. From a brain networks perspective, rule inference requires the activation of regions of the attention network, possibly reflecting the continuous need for attention control over different types of interference/stimuli/activity, both endogenous (e.g. elaboration of rules, hypothesis testing) and exogenous (e.g. elaboration of new stimuli/features). Regions of the attention network might play a role in attentional control in response to cues relevant for understanding the rule governing each trial, as well as during performance feedback on a trial-by-trial basis (to improve inference strategies across trials)(Dosenbach et al., 2007; Fair et al., 2007). When the rule characterizing a trial has been identified (e.g. Boolean operator AND), the need for rule and task set maintenance becomes a priority in order to generate new answers based on the recent insight. As a consequence, resources for additional hypothesis testing are constrained and the suppression of distractors becomes priority: such "inhibition" might be possibly expressed by activity of the Anterior Salience network nodes as highlighted by the anatomical mapping, including major roles for the insula, dorsal ACC and the thalamus.

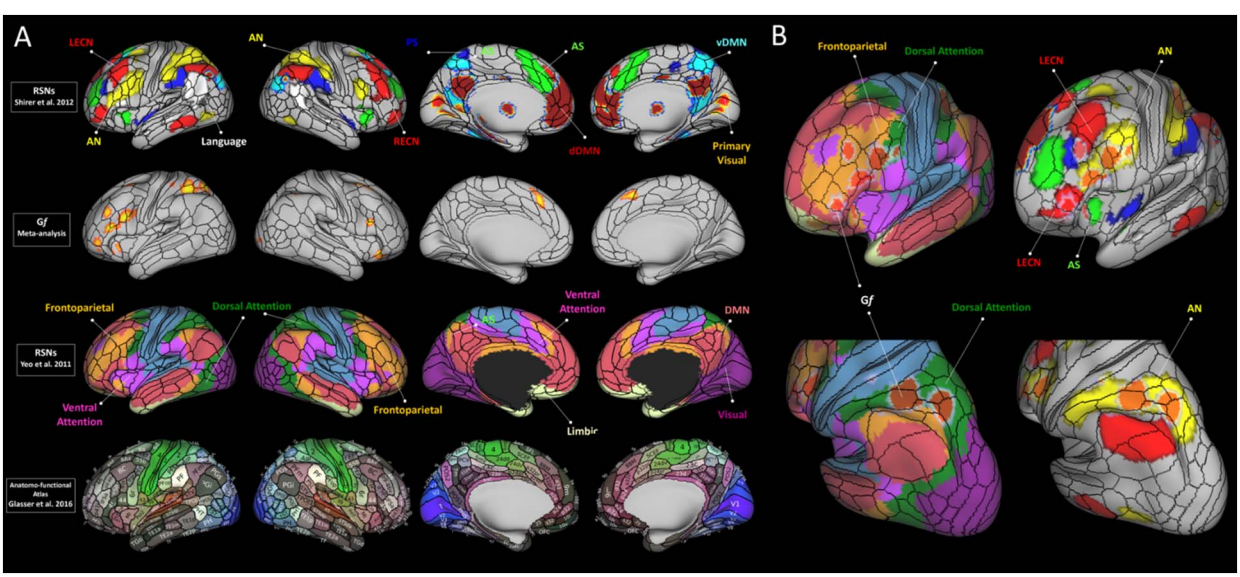

Fig. 8. G*f* and resting-state networks. Surface representations of RSNs identified by Shirer et al. (2012) and Yeo et al. (2011) showing the highest overlap with G*f* maps are shown (A), together with the overall G*f* map nodes and the novel multimodal brain parcellation scheme recently published by Glasser et al. (2016). As quantified in Fig. 7, the overlap between G*f* regions (red blobs) and nodes of the attention network is evident especially in the parietal lobes, with additional contributions by regions of the AS and LECN in the prefrontal ones. A more detailed comparison of the overlap between prefrontal and parietal G*f* nodes with available RSN parcellations is also shown (B). Only those networks showing overlap with G*f* are labeled. Note: AS = anterior salience network; AN = attention network; LECN = left executive control network; vDMN = ventral Default mode network; dDMN = dorsal default mode network; PS = posterior salience network. (For interpretation of the references to colour in this figure legend, the reader is referred to the web version of this article.)

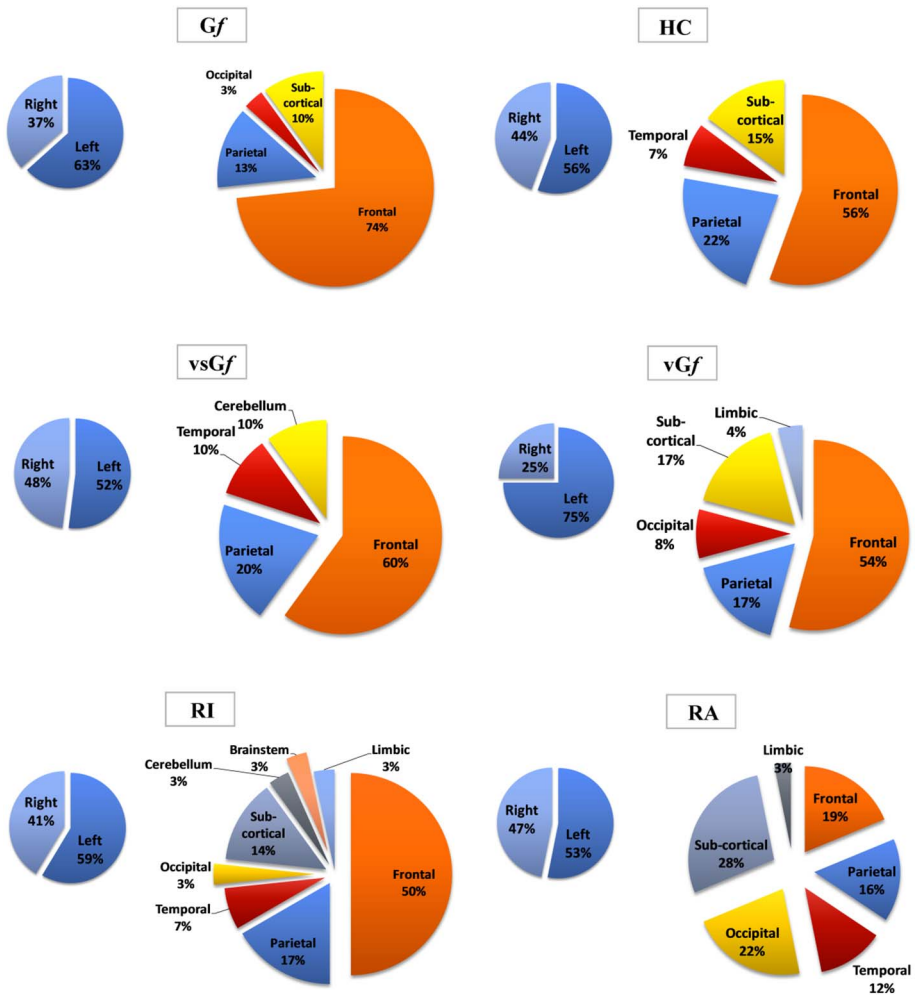

Fig. 9. Lateralization and Lobar distribution. For each significant cluster included in the ALE maps, the percentage of activations being reported in left and right hemisphere are shown, as well as the distribution of activation across cerebral lobes, brainstem and cerebellum. Values have been calculated as the ratio between the label assigned to each ALE map cluster (e.g. prefrontal) and the total number of significant clusters in each ALE map. A direct comparison of values in two different plots is not suggested.

4.1.3. Subcortical Gf

Our maps highlight a significant contribution of subcortical structures during G*f*-related processing. While surprising for its extent and relevance in almost all the different G*f* maps, previous evidence have stressed such link (Wartenburger, Heekeren, Preusse, Kramer, & van der Meer, 2009), reporting correlations between G*f* and the morphology of right striatum structures (i.e. caudate nucleus, putamen, and nucleus accumbens)(Burgaleta et al., 2014), the caudate nuclei (Rhein et al., 2014)(Melrose, Poulin, & Stern, 2007) and ventral striatum (Schlagenhauf et al., 2013). Numerous studies have also documented association between morphology/functional profile of subcortical structures and cognitive functions other than G*f*: working memory (Cools, Gibbs, Miyakawa, Jagust, & D'Esposito, 2008; Landau, Lal, O'Neil, Baker, & Jagust, 2009), inhibition (Li, Yan, Sinha, & Lee, 2008), verbal and spatial memory (Moffat, Kennedy, Rodrigue, & Raz, 2007)(Maguire et al., 1998), language processing (Abdullaev, Bechtereva & Melnichuk, 1998) and arithmetic (Dehaene et al., 1996). Interestingly, different structures of the basal ganglia express their connections with cortical areas according to their position, with rostral-central parts–important for working memory and higher order cognition—being more connected to prefrontal structures (Martinez et al., 2003; Postuma & Dagher, 2006), while central-caudal segments showing more links with parietal and parieto-occipital cortices involved in spatial processing (Jordan, Wustenberg, Heinze, Peters, & Jancke, 2002). A careful anatomical and functional mapping of the activation foci highlighted in the present work might help elucidate the differential contribution of Basal Ganglia structures shown in multiple G*f* maps, such as vG*f*, HC and Rule Application.

4.1.4. Improving targeting for cognitive enhancement

Noninvasive brain stimulation (NIBS), and transcranial electrical stimulation (tES) in particular, are becoming pivotal tools for the investigations of cognitive enhancement solutions in healthy young and elderly humans (Santarnecchi et al., 2015a)(Filmer, Dux, & Mattingley, 2014)(Tatti, Rossi, Innocenti, Rossi, & Santarnecchi, 2016). The possibility of applying low voltage electrical stimulation patterns to modulate–excite or inhibit—the activity of specific brain regions or entire networks constitutes an appealing scenario (e.g. using transcranial direct current stimulation, tDCS)(Nitsche & Paulus, 2011), with potential applications for both the causal investigation of brain-function dualism (following the "virtual-lesion" approach (Pascual-Leone & Hallett, 1994; Pascual-Leone & Pridmore, 1995), as well as for the enhancement of individual cognitive functioning (E. Santarnecchi, Muller, Sarkar, Polizzotto, & Cohen Kadosh, 2016; Emiliano Santarnecchi et al., 2013)(Polania, Nitsche, Korman, Batsikadze, & Paulus, 2012; Sela, Kilim, & Lavidor, 2012; Snowball et al., 2013). Additionally, recently developed techniques such as transcranial alternating current (tACS) and transcranial random noise (tRNS) stimulation offers the possibility to modulate brain activity by interacting with specific brain oscillatory dynamics as those recorded via electroencephalography (EEG), thus exponentially multiplying potentially available interventions (Thut, Miniussi, & Gross, 2012).

In this framework, with the increasing spatial resolution of tES modeling approaches (Datta et al., 2009) and the possibility to indirectly stimulate subcortical structure using TMS (Wang et al., 2014), "how" to stimulate specific neural substrates is becoming a less relevant question, whereas "where" to stimulate is probably the most relevant issue for the implementation of effective cognitive enhancement protocols. Here we showed how the different sub-networks composing the neural substrate of G*f* in humans appears to be all but spatially homogeneous or easily linkable to just a few brain regions. Current neuromodulatory protocols aimed at increasing intelligence have shown promising results by means of interventions focused on the stimulation of one single region, such as the left middle frontal gyrus (Santarnecchi et al., 2016)(Santarnecchi et al., 2013) or the left parietal lobe (Pahor & Jausovec, 2014), while attempts at increasing working memory has been carried out also by synchronizing/desynchronizing a small network (Polania et al., 2012). Our maps show how this is nonetheless a reductive argument towards the idea of increasing G*f*, whose network seems to include approximately 16 nodes. Most importantly, the comparison of activations related to rule inference and rule application shows no clear overlap, with specific areas supporting one or the other process at different stages of processing. this also suggests a need to revisit the working principles of cognitive enhancement studies based on NIBS published so far, where no distinction between these processes was made and the stimulation took place during the entire problem-solving process. Such low temporal specificity could have dramatically reduced the impact of NIBS interventions, or even counteracted their efficacy by stimulating brain regions whose activity was not specifically required during specific phases.

Future studies might use fMRI activation maps to inform NIBS paradigms and create stimulation solutions resembling the sub-network (s) of interest for the specific function/processing stage at hand (Ruffini, Fox, Ripolles, Miranda, & Pascual-Leone, 2014), or aim for regions activated across domains/functions to favor transfer during cognitive training.

4.1.5. Relevance for cognitive training and transfer of effects

Recent investigations have shown the possibility of increasing individual G*f* capacity by means of cognitive training interventions tailored around the evidence of functional overlap between G*f* and executive functions (Au et al., 2014). Even though such results are controversial (Moody, 2009), training these functions–especially working memory—has been shown to induce changes in G*f* scores after training, albeit with small to moderate effect sizes (Au et al., 2014). However, no clear quantification of the neuroanatomical and functional overlap between G*f* and the functions being trained is available to date, making the quest for transfer effects a reasonable argument at the behavioral/psychometric level (R. Colom, Jung, & Haier, 2006), but a speculative one at the neurobiological one (R.J. Haier, 2014). Most importantly, how the aforementioned overlap between functions being trained (e.g. WM, inhibition, switch) and the target functions (e.g. G*f*) before training might shape the impact of the training itself remains another absolutely relevant, unanswered question. Given the variability in the sub-networks identified in the present meta-analysis, it is likely that different executive functions will load differently on G*f* maps, with potentially interesting interactions (e.g. switching and working memory might be more related to rule inference processes where multiple alternative explanations are validated under time pressure, while inhibition might help holding relevant information during the rule application phase). This theoretical framework can help select the best function to be trained in relation to the specific transfer effect being pursued. The interplay between the nodes of each network could also be tested using functional connectivity analysis, in order to identify potential anatomo-functional associations between cognitive modules involved in the training and/or the target functions (Expert, Evans, Blondel, & Lambiotte, 2011).

Interestingly, in discussing theories and models of "far" cognitive transfer, Greenwood and Parasuraman have recently proposed a pivotal role for the attention network: starting from the shielding role against interference played by focal attention towards items held in WM suggested by Cowan et al. (Cowan, 2001), the authors suggest that any training aimed at inducing far transfer effects (including those on G*f*) might primarily focus on–explicitly or implicitly—increase individual ability to ignore distractors (e.g., working memory training and perceptual training), a core function of the attention and frontoparietal control networks (Greenwood & Parasuraman, 2016). Additional evidence in children (5 years old, $n = 37$) also suggests that attention-based training induces changes at both behavioral and EEG level, with increased fronto-parietal connectivity and transfer to G*f* (Rueda, Checa, & Combita, 2012). In this context, the concept of attention training could benefit of the association between G*f* and specific nodes of the ventral and dorsal Attention Network, leading to protocols maximizing the recruitment of these regions.

5. Conclusion

As recently suggested (R. Colom, Karama, Jung, & Haier, 2010), the quest for the neurobiological underpinnings of (*fluid*) intelligence must merge with the brain connectivity literature to fulfill its purpose. Apart from a precise anatomical localization and labeling of specific activation foci, our data promote a network-centered view of G*f*-related problem solving, suggesting an intriguing overlap with regions of the attention network, with additional contributions by regions related to salience processing and cognitive control.

Financial disclosures

All authors report no conflict of interest.

Acknowledgement

This research is based upon work supported by the Office of the Director of National Intelligence (ODNI), Intelligence Advanced Research Projects Activity (IARPA), via 2014-13121700007. The views and conclusions contained herein are those of the authors and should not be interpreted as necessarily representing the official policies or endorsements, either expressed or implied, of the ODNI, IARPA, or the U.S. Government. The U.S. Government is authorized to reproduce and distribute reprints for Governmental purposes notwithstanding any copyright annotation thereon. Dr. Pascual-Leone is further supported by the Berenson-Allen Foundation, the Sidney R. Baer Jr. Foundation, grants from the National Institutes of Health (R01HD069776, R01NS073601, R21 MH099196, R21 NS082870, R21 NS085491, R21 HD07616), and Harvard Catalyst, The Harvard Clinical and Translational Science Center (NCRR and the NCATS NIH, UL1 RR025758). The content of this paper is solely the responsibility of the authors and does not necessarily represent the official views of Harvard Catalyst, Harvard University and its affiliated academic health care centers, the National Institutes of Health, the Sidney R. Baer Jr. Foundation. The authors would like to thank the members of the larger Honeywell SHARP team for their valuable contributions to this work, including the SHARP Team authors:Harvard Medical School (Ann Connor, Franziska Plessow, Sadhvi Saxena, Erica Levenbaum); Honeywell (Jessamy Almquist, Michael Dillard, Umut Orhan, Santosh Mathan); Northeastern University (James McKanna, Deniz Erdogmus, Misha Pavel); Oxford University (Anna-Katharine Brem, Roi Cohen Kadosh, Nick Yeung); SimCoach Games (Garrett Kimball, Eben Myers).

References

Abdullaev, Y. G., Bechtereva, N. P., & Melnichuk, K. V. (1998). Neuronal activity of human caudate nucleus and prefrontal cortex in cognitive tasks. *Behavioural Brain*

Research, 97(1–2), 159–177.
Achard, S., & Bullmore, E. (2007). Efficiency and Cost of Economical Brain Functional Networks. *PLoS Computational Biology*, *3*(2), e17. http://dx.doi.org/10.1371/journal.pcbi.0030017.
Adelstein, J. S., Shehzad, Z., Mennes, M., Deyoung, C. G., Zuo, X. N., Kelly, C., Margulies, D. S., et al. (2011). Personality Is Reflected in the Brain's Intrinsic Functional Architecture. *PloS One*, *6*(11), e27633. http://dx.doi.org/10.1371/journal.pone.0027633.
Agosta, F., Pievani, M., Geroldi, C., Copetti, M., Frisoni, G. B., & Filippi, M. (2012). Resting state fMRI in Alzheimer's disease: Beyond the default mode network. *Neurobiology of Aging*, *33*(8), 1564–1578. http://dx.doi.org/10.1016/j.neurobiolaging.2011.06.007.
Allen, E. A., Damaraju, E., Plis, S. M., Erhardt, E. B., Eichele, T., & Calhoun, V. D. (2014). Tracking whole-brain connectivity dynamics in the resting state. *Cerebral Cortex*, *24*(3), 663–676. http://dx.doi.org/10.1093/cercor/bhs352.
Au, J., Sheehan, E., Tsai, N., Duncan, G. J., Buschkuehl, M., & Jaeggi, S. M. (2014). Improving fluid intelligence with training on working memory: A meta-analysis. *Psychonomic Bulletin & Review*, 1531–5320. http://dx.doi.org/10.3758/s13423-014-0699-x (Electronic, August).
Baltes, P. B., Staudinger, U. M., & Lindenberger, U. (1999). Lifespan psychology: Theory and application to intellectual functioning. *Annual Review of Psychology*, *50*, 0066–4308. 471–507 http://dx.doi.org/10.1146/annurev.psych.50.1.471 (Print) .
Barbey, A. K., Colom, R., Solomon, J., Krueger, F., Forbes, C., & Grafman, J. (2012). An integrative architecture for general intelligence and executive function revealed by lesion mapping. *Brain*, *135*(Pt 4), 1154–1164. http://dx.doi.org/10.1093/brain/aws021.
Barbey, A. K., Colom, R., Paul, E. J., & Grafman, J. (2014). Architecture of fluid intelligence and working memory revealed by lesion mapping. *Brain Structure & Function*, *219*(2), 485–494. http://dx.doi.org/10.1007/s00429-013-0512-z.
Bassett, D. S., Bullmore, E., Verchinski, B. A., Mattay, V. S., Weinberger, D. R., & Meyer-Lindenberg, A. (2008). Hierarchical organization of human cortical networks in health and schizophrenia. *The Journal of Neuroscience*, *28*(37), 9239–9248. http://dx.doi.org/10.1523/JNEUROSCI.1929-08.2008.
Bestmann, S., de Berker, A. O., & Bonaiuto, J. (2015). Understanding the behavioural consequences of noninvasive brain stimulation. *Trends in Cognitive Sciences*, *19*, 13–20. http://dx.doi.org/10.1016/j.tics.2014.10.003 (1879–307X (Electronic)).
Biswal, B. B., Mennes, M., Zuo, X. N., Gohel, S., Kelly, C., Smith, S. M., Beckmann, C. F., et al. (2010). Toward discovery science of human brain function. *Proceedings of the National Academy of Sciences of the United States of America*, *107*(10), 4734–4739. http://dx.doi.org/10.1073/pnas.0911855107.
Bonavita, S., Sacco, R., Esposito, S., d'Ambrosio, A., Della, C. M., Corbo, D., Docimo, R., et al. (2016). Default mode network changes in multiple sclerosis: A link between depression and cognitive impairment? *European Journal of Neurology*. no. 1468–1331 (Electronic) (September) http://dx.doi.org/10.1111/ene.13112.
Botvinick, M., Nystrom, L. E., Fissell, K., Carter, C. S., & Cohen, J. D. (1999). Conflict monitoring versus selection-for-action in anterior cingulate cortex. *Nature*, *402*(6758), 179–181. http://dx.doi.org/10.1038/46035.
Botvinick, M. M., Braver, T. S., Barch, D. M., Carter, C. S., & Cohen, J. D. (2001). Conflict monitoring and cognitive control. *Psychological Review*, *108*(3), 624–652.
Botvinick, M. M., Cohen, J. D., & Carter, C. S. (2004). Conflict monitoring and anterior cingulate cortex: An update. *Trends in Cognitive Sciences*, *8*(12), 539–546. http://dx.doi.org/10.1016/j.tics.2004.10.003.
Braun, U., Plichta, M. M., Esslinger, C., Sauer, C., Haddad, L., Grimm, O., Mier, D., et al. (2012). Test–retest reliability of resting-state connectivity network characteristics using fMRI and graph theoretical measures. *NeuroImage*, *59*(2), 1404–1412. http://dx.doi.org/10.1016/j.neuroimage.2011.08.044.
Braver, T. S., & Barch, D. M. (2006). Extracting core components of cognitive control. *Trends in Cognitive Sciences*, *10*(12), 529–532. http://dx.doi.org/10.1016/j.tics.2006.10.006.
Bundesen, C. (1990). A theory of visual attention. *Psychological Review*, *97*(4), 523–547.
Bunge, S. A., Wallis, J. D., Parker, A., Brass, M., Crone, E. A., Hoshi, E., & Sakai, K. (2005). Neural circuitry underlying rule use in humans and nonhuman primates. *The Journal of Neuroscience*, *25*(45), 10347–10350. http://dx.doi.org/10.1523/JNEUROSCI.2937-05.2005.
Burgaleta, M., MacDonald, P. A., Martinez, K., Roman, F. J., Alvarez-Linera, J., Ramos, G. A., ... Colom, R. (2014). Subcortical regional morphology correlates with fluid and spatial intelligence. *Human Brain Mapping*, *35*(5), 1957–1968. http://dx.doi.org/10.1002/hbm.22305.
Carter, C. S., Braver, T. S., Barch, D. M., Botvinick, M. M., Noll, D., & Cohen, J. D. (1998). Anterior cingulate cortex, error detection, and the online monitoring of performance. *Science*, *280*(5364), 747–749.
Cattel, R. B. (1963). Theory of fluid and crystallized intelligence: A critical experiment. *Journal of Educational Psychology*, *54*(1), http://dx.doi.org/10.1016/j.neuroimage.2010.06.016.
Choe, Ann S., Craig K. Jones, Suresh E. Joel, John Muschelli, Visar Belegu, Brian S. Caffo, Martin A. Lindquist, Peter C. M. van Zijl, and James J. Pekar. 2015. "Reproducibility and temporal structure in weekly resting-state fMRI over a period of 3.5 years." Edited by Daniel Margulies. PloS One 10 (10): e0140134. doi:http://dx.doi.org/10.1371/journal.pone.0140134.
Christoff, K., Prabhakaran, V., Dorfman, J., Zhao, Z., Kroger, J. K., Holyoak, K. J., & Gabrieli, J. D. (2001). Rostrolateral prefrontal cortex involvement in relational integration during reasoning. *NeuroImage*, *14*(5), 1136–1149. http://dx.doi.org/10.1006/nimg.2001.0922.
Chuderski, A., & Necka, E. (2012). The contribution of working memory to fluid reasoning: Capacity, control, or both? *Journal of Experimental Psychology: Learning, Memory, and Cognition*, *38*(6), 1689–1710. http://dx.doi.org/10.1037/a0028465.
Cocchi, L., Halford, G. S., Zalesky, A., Harding, I. H., Ramm, B. J., Cutmore, T., ... Mattingley, J. B. (2014). Complexity in relational processing predicts changes in functional brain network dynamics. *Cerebral Cortex*, *24*(9), 2283–2296. http://dx.doi.org/10.1093/cercor/bht075.
Cole, M. W., Yarkoni, T., Repovs, G., Anticevic, A., & Braver, T. S. (2012). Global connectivity of prefrontal cortex predicts cognitive control and intelligence. *The Journal of Neuroscience*, *32*(26), 8988–8999. http://dx.doi.org/10.1523/JNEUROSCI.0536-12.2012.
Colom, R., Jung, R. E., & Haier, R. J. (2006). Distributed brain sites for the G-factor of intelligence. *NeuroImage*, *31*(3), 1359–1365. http://dx.doi.org/10.1016/j.neuroimage.2006.01.006.
Colom, R., Haier, R. J., Head, K., Alvarez-Linera, J., Quiroga, M. A., Shih, P. C., & Jung, R. E. (2009). Gray matter correlates offluid, crystallized, and spatial intelligence: Testing the P-FIT model. *Intelligence*, *37*(4), 124–135.
Colom, R., Karama, S., Jung, R. E., & Haier, R. J. (2010). Human intelligence and brain networks. *Dialogues in Clinical Neuroscience*, *12*(4), 489–501.
Colom, R., Burgaleta, M., Roman, F. J., Karama, S., Alvarez-Linera, J., Abad, F. J., ... Haier, R. J. (2013a). Neuroanatomic overlap between intelligence and cognitive factors: Morphometry methods provide support for the key role of the frontal lobes. *NeuroImage*, *72C*, 143–152. http://dx.doi.org/10.1016/j.neuroimage.2013.01.032 (1095–9572 (Electronic)).
Colom, R., M. Burgaleta, F.J. Roman, S. Karama, J. Alvarez-Linera, F.J. Abad, K. Martinez, M.A. Quiroga, and R.J. Haier. 2013b. "Neuroanatomic overlap between intelligence and cognitive factors: Morphometry methods provide support for the key role of the frontal lobes." NeuroImage 72: 143–52. doi:http://dx.doi.org/10.1016/j.neuroimage.2013.01.032 (1095–9572 (Electronic)).
Colom, R., Hua, X., Martinez, K., Burgaleta, M., Roman, F. J., Gunter, J. L., ... Thompson, P. M. (2016a). Brain structural changes following adaptive cognitive training assessed by tensor-based morphometry (TBM). *Neuropsychologia*, *91*, 77–85. http://dx.doi.org/10.1016/j.neuropsychologia.2016.07.034 (1873–3514 (Electronic)).
Colom, R., Chuderski, A., & Santarnecchi, E. (2016b). Bridge over troubled water: Commenting on Kovacs and Conway's process overlap theory. *Psychological Inquiry*, *27*(3), 181–189. http://dx.doi.org/10.1080/1047840X.2016.1181513.
Cools, R., Gibbs, S. E., Miyakawa, A., Jagust, W., & D'Esposito, M. (2008). Working memory capacity predicts dopamine synthesis capacity in the human striatum. *The Journal of Neuroscience*, *28*(5), 1208–1212. http://dx.doi.org/10.1523/JNEUROSCI.4475-07.2008.
Corbetta, M., Patel, G., & Shulman, G. L. (2008). The reorienting system of the human brain: From environment to theory of mind. *Neuron*, *58*(3), 306–324. http://dx.doi.org/10.1016/j.neuron.2008.04.017.
Cowan, N. (2001). The magical number 4 in short-term memory: A reconsideration of mental storage capacity. *Behavioral and Brain Sciences*, *24*(1), 87–114. http://dx.doi.org/10.1017/S0140525X01003922.
Craighero, L., Bello, A., Fadiga, L., & Rizzolatti, G. (2002). Hand action preparation influences the responses to hand pictures. *Neuropsychologia*, *40*(5), 492–502.
Crottaz-Herbette, S., & Menon, V. (2006). Where and when the anterior cingulate cortex modulates attentional response: Combined fMRI and ERP evidence. *Journal of Cognitive Neuroscience*, *18*(5), 766–780. http://dx.doi.org/10.1162/jocn.2006.18.5.766.
Datta, A., Bansal, V., Diaz, J., Patel, J., Reato, D., & Bikson, M. (2009). Gyri-precise head model of transcranial direct current stimulation: Improved spatial focality using a ring electrode versus conventional rectangular pad. *Brain Stimulation*, *2*, 201–207. http://dx.doi.org/10.1016/j.brs.2009.03.005 (1935–861X (Print)).
Deary, I. (2008). Why do intelligent people live longer? *Nature*, *456*(7219), 175–176. http://dx.doi.org/10.1038/456175a.
Dehaene, S., Tzourio, N., Frak, V., Raynaud, L., Cohen, L., Mehler, J., & Mazoyer, B. (1996). Cerebral activations during number multiplication and comparison: a PET study. *Neuropsychologia*, *34*(11), 1097–1106.
Desimone, R., & Duncan, J. (1995). Neural mechanisms of selective visual attention. *Annual Review of Neuroscience*, *18*, 193–222. http://dx.doi.org/10.1146/annurev.ne.18.030195.001205 (0147–006X (Print)).
Dietrich, A., & Kanso, R. (2010). A Review of EEG, ERP, and neuroimaging studies of creativity and insight. *Psychological Bulletin*, *136*, 822–848. http://dx.doi.org/10.1037/a0019749 (1939–1455 (Electronic)).
Dosenbach, N. U., Visscher, K. M., Palmer, E. D., Miezin, F. M., Wenger, K. K., Kang, H. C., ... Petersen, S. E. (2006). A core system for the implementation of task sets. *Neuron*, *50*(5), 799–812. http://dx.doi.org/10.1016/j.neuron.2006.04.031.
Dosenbach, N. U., Fair, D. A., Miezin, F. M., Cohen, A. L., Wenger, K. K., Dosenbach, R. A., Fox, M. D., et al. (2007). Distinct brain networks for adaptive and stable task control in humans. *Proceedings of the National Academy of Sciences of the United States of America*, *104*(26), 11073–11078. http://dx.doi.org/10.1073/pnas.0704320104.
Dosenbach, N. U., Fair, D. A., Cohen, A. L., Schlaggar, B. L., & Petersen, S. E. (2008). A dual-networks architecture of top-down control. *Trends in Cognitive Sciences*, *12*(3), 99–105. http://dx.doi.org/10.1016/j.tics.2008.01.001.
Downing, P. E. (2000). Interactions between visual working memory and selective attention. *Psychological Science*, *11*(6), 467–473.
Ebisch, S. J., Perrucci, M. G., Mercuri, P., Romanelli, R., Mantini, D., Romani, G. L., ... Saggino, A. (2012). Common and unique neuro-functional basis of induction, visualization, and spatial relationships as cognitive components of fluid intelligence. *NeuroImage*, *62*(1), 331–342. http://dx.doi.org/10.1016/j.neuroimage.2012.04.053.
Eickhoff, S. B., Laird, A. R., Grefkes, C., Wang, L. E., Zilles, K., & Fox, P. T. (2009). Coordinate-based activation likelihood estimation meta-analysis of neuroimaging data: A random-effects approach based on empirical estimates of spatial uncertainty. *Human Brain Mapping*, *30*, 2907–2926. http://dx.doi.org/10.1002/hbm.20718 (1097–0193 (Electronic)).

Eickhoff, S. B., Bzdok, D., Laird, A. R., Kurth, F., & Fox, P. T. (2012). Activation likelihood estimation meta-analysis revisited. *NeuroImage*, *59*, 2349–2361. http://dx.doi.org/10.1016/j.neuroimage.2011.09.017 (1095–9572 (Electronic)).

Escorial, S., Roman, F. J., Martinez, K., Burgaleta, M., Karama, S., & Colom, R. (2015). Sex differences in neocortical structure and cognitive performance: A surface-based morphometry study. *NeuroImage*, *104*, 355–365. http://dx.doi.org/10.1016/j.neuroimage.2014.09.035 (1095–9572 (Electronic)).

Etkin, A., Egner, T., Peraza, D. M., Kandel, E. R., & Hirsch, J. (2006). Resolving emotional conflict: A role for the rostral anterior cingulate cortex in modulating activity in the amygdala. *Neuron*, *51*(6), 871–882. http://dx.doi.org/10.1016/j.neuron.2006.07.029.

Expert, P., Evans, T. S., Blondel, V. D., & Lambiotte, R. (2011). Uncovering space-independent communities in spatial networks. *Proceedings of the National Academy of Sciences of the United States of America*, *108*(19), 7663–7668. http://dx.doi.org/10.1073/pnas.1018962108.

Fair, D. A., Dosenbach, N. U., Church, J. A., Cohen, A. L., Brahmbhatt, S., Miezin, F. M., ... Schlaggar, B. L. (2007). Development of distinct control networks through segregation and integration. *Proceedings of the National Academy of Sciences of the United States of America*, *104*(33), 13507–13512. http://dx.doi.org/10.1073/pnas.0705843104.

Filmer, H. L., Dux, P. E., & Mattingley, J. B. (2014). Applications of transcranial direct current stimulation for understanding brain function. *Trends in Neurosciences*, *37*, 742–753. http://dx.doi.org/10.1016/j.tins.2014.08.003 (1878–108X (Electronic)).

Finn, E. S., Shen, X., Scheinost, D., Rosenberg, M. D., Huang, J., Chun, M. M., ... Constable, R. T. (2015). Functional connectome fingerprinting: Identifying individuals using patterns of brain connectivity. *Nature Neuroscience*, *18*(11), 1664–1671. http://dx.doi.org/10.1038/nn.4135.

Fox, M. D., Snyder, A. Z., Vincent, J. L., Corbetta, M., Van Essen, D. C., & Raichle, M. E. (2005). The human brain is intrinsically organized into dynamic, anticorrelated functional networks. *Proceedings of the National Academy of Sciences of the United States of America*, *102*(27), 9673–9678. http://dx.doi.org/10.1073/pnas.0504136102.

Geake, J. G., & Hansen, P. C. (2005). Neural correlates of intelligence as revealed by fMRI of fluid analogies. *NeuroImage*, *26*(2), 555–564. http://dx.doi.org/10.1016/j.neuroimage.2005.01.035.

Geake, J. G., & Hansen, P. C. (2010). Functional neural correlates of fluid and crystallized analogizing. *NeuroImage*, *49*(4), 3489–3497. http://dx.doi.org/10.1016/j.neuroimage.2009.09.008.

Glasser, M. F., Coalson, T. S., Robinson, E. C., Hacker, C. D., Harwell, J., Yacoub, E., Ugurbil, K., et al. (2016). A multi-modal parcellation of human cerebral cortex. *Nature*, *536*(7615), 171–178. http://dx.doi.org/10.1038/nature18933.

Goel, V., Buchel, C., Frith, C., & Dolan, R. J. (2000). Dissociation of mechanisms underlying syllogistic reasoning. *NeuroImage*, *12*(5), 504–514. http://dx.doi.org/10.1006/nimg.2000.0636.

Golde, M., von Cramon, D. Y., & Schubotz, R. I. (2010). Differential role of anterior prefrontal and premotor cortex in the processing of relational information. *NeuroImage*, *49*(3), 2890–2900. http://dx.doi.org/10.1016/j.neuroimage.2009.09.009.

Gray, J. R., Chabris, C. F., & Braver, T. S. (2003). Neural mechanisms of general fluid intelligence. *Nature Neuroscience*, *6*(3), 316–322. http://dx.doi.org/10.1038/nn1014.

Green, A. E., Fugelsang, J. A., Kraemer, D. J. M., Shamosh, N. A., & Dunbar, K. N. (2006). Frontopolar cortex mediates abstract integration in analogy. *Brain Research*, *1096*(1), 125–137. http://dx.doi.org/10.1016/j.brainres.2006.04.024.

Greenwood, P. M., & Parasuraman, R. (2016). The mechanisms of far transfer from cognitive training: Review and hypothesis. *Neuropsychology*, *30*(6), 742–755. http://dx.doi.org/10.1037/neu0000235.

Haier, R. J. (2014). Increased intelligence is a myth (so far). *Frontiers in Systems Neuroscience*, *8*(34), http://dx.doi.org/10.3389/fnsys.2014.00034 (1662–5137 (Electronic)).

Haier, R. J., Siegel, B. V., Nuechterlein, K. H., Hazlett, E., Wu, J. C., Paek, J., ... Buchsbaum, M. S. (1988). Cortical glucose metabolic-rate correlates of abstract reasoning and attention studied with positron emission tomography. *Intelligence*, *12*, 199–217. http://dx.doi.org/10.1186/1756-0500-3-206 (1756–0500 (Electronic)).

Haier, R. J., Siegel, B., Tang, C., Abel, L., & Buchsbaum, M. S. (1992). Intelligence and changes in regional cerebral glucose metabolic rate following learning. *Intelligence*, *16*(3–4), 415–426. http://dx.doi.org/10.1016/0160-2896(92)90018-M.

Hossiep, R., Turck, D., & Hasella, M. (1999). Bochumer Matrizentest: BOMAT advanced-short version. *Göttingen*. http://dx.doi.org/10.1016/j.neuroimage.2010.06.016 no. 1095–9572 (Electronic) (October).

Houde, O. (2010). Beyond IQ comparisons: Intra-individual training differences. *Nature Reviews. Neuroscience*, *11*(5), 370. http://dx.doi.org/10.1038/nrn2793-c1.

Jordan, K., Wustenberg, T., Heinze, H. J., Peters, M., & Jancke, L. (2002). Women and men exhibit different cortical activation patterns during mental rotation tasks. *Neuropsychologia*, *40*(13), 2397–2408.

Jung, R. E., & Haier, R. J. (2007). The Parieto-frontal integration theory (P-FIT) of intelligence: Converging neuroimaging evidence. *The Behavioral and Brain Sciences*, *30*(2), 135–154. http://dx.doi.org/10.1017/S0140525X07001185.

Krawczyk, D. C. (2012). The cognition and neuroscience of relational reasoning. *Brain Research*, *1428*, 13–23. http://dx.doi.org/10.1016/j.brainres.2010.11.080 (1872–6240 (Electronic)).

Krawczyk, D. C., Michelle, M. C. M., & Donovan, C. M. (2011). A hierarchy for relational reasoning in the prefrontal cortex. *Cortex*, *47*, 588–597. http://dx.doi.org/10.1016/j.cortex.2010.04.008 (1973–8102 (Electronic)).

Landau, S. M., Lal, R., O'Neil, J. P., Baker, S., & Jagust, W. J. (2009). Striatal dopamine and working memory. *Cerebral Cortex*, *19*(2), 445–454. http://dx.doi.org/10.1093/cercor/bhn095.

Li, C. S., Yan, P., Sinha, R., & Lee, T. W. (2008). Subcortical processes of motor response inhibition during a stop signal task. *NeuroImage*, *41*(4), 1352–1363. http://dx.doi.org/10.1016/j.neuroimage.2008.04.023.

Lindell, A. K. (2011). Lateral thinkers are not so laterally minded: Hemispheric asymmetry, interaction, and creativity. *Laterality*, *16*(4), 479–498. http://dx.doi.org/10.1080/1357650X.2010.497813.

Luo, Q., Perry, C., Peng, D., Jin, Z., Xu, D., Ding, G., & Xu, S. (2003). The neural substrate of analogical reasoning: An fMRI study. *Brain Research. Cognitive Brain Research*, *17*(3), 527–534.

Maguire, E. A., Burgess, N., Donnett, J. G., Frackowiak, R. S., Frith, C. D., & O'Keefe, J. (1998). Knowing where and getting there: A human navigation network. *Science*, *280*(5365), 921–924.

Martinez, D., Slifstein, M., Broft, A., Mawlawi, O., Hwang, D. R., Huang, Y., Cooper, T., et al. (2003). Imaging human mesolimbic dopamine transmission with positron emission tomography. Part II: Amphetamine-induced dopamine release in the functional subdivisions of the striatum. *Journal of Cerebral Blood Flow and Metabolism*, *23*(3), 285–300.

Matzen, L. E., Benz, Z. O., Dixon, K. R., Posey, J., Kroger, J. K., & Speed, A. E. (2010). Recreating Raven's: Software for systematically generating large numbers of Raven-like matrix problems with normed properties. *Behavior Research Methods*, *42*, 525–541. http://dx.doi.org/10.3758/BRM.42.2.525 (1554–3528 (Electronic)).

Melrose, R. J., Poulin, R. M., & Stern, C. E. (2007). An fMRI investigation of the role of the basal ganglia in reasoning. *Brain Research*, *1142*, 146–158. http://dx.doi.org/10.1016/j.brainres.2007.01.060 (0006–8993 (Print)).

Miyake, A., & Friedman, N. P. (2012). The nature and organization of individual differences in executive functions: Four general conclusions. *Current Directions in Psychological Science*, *21*(1), 8–14. http://dx.doi.org/10.1177/0963721411429458.

Miyake, A., Friedman, N. P., Emerson, M. J., Witzki, A. H., Howerter, A., & Wager, T. D. (2000). The unity and diversity of executive functions and their contributions to complex 'frontal lobe' tasks: A latent variable analysis. *Cognitive Psychology*, *41*(1), 49–100. http://dx.doi.org/10.1006/cogp.1999.0734.

Moffat, S. D., Kennedy, K. M., Rodrigue, K. M., & Raz, N. (2007). Extrahippocampal contributions to age differences in human spatial navigation. *Cerebral Cortex*, *17*(6), 1274–1282. http://dx.doi.org/10.1093/cercor/bhl036.

Moody, D. E. (2009). Can intelligence be increased by training on a task of working memory? *Intelligence*, *37*(4), 327–328. http://dx.doi.org/10.1016/j.intell.2009.04.005.

Moore, T., & Armstrong, K. M. (2003). Selective gating of visual signals by microstimulation of frontal cortex. *Nature*, *421*(6921), 370–373. http://dx.doi.org/10.1038/nature01341.

Nikolaidis, A., Baniqued, P. L., Kranz, M. B., Scavuzzo, C. J., Barbey, A. K., Kramer, A. F., & Larsen, R. J. (2016). Multivariate associations of fluid intelligence and NAA. *Cerebral Cortex*. no. 1460–2199 (Electronic) (March) http://dx.doi.org/10.1093/cercor/bhw070.

Nitsche, M. A., & Paulus, W. (2011). Transcranial direct current stimulation—Update 2011. *Restorative Neurology and Neuroscience*, *29*, 463–492. http://dx.doi.org/10.3233/RNN-2011-0618 (1878–3627 (Electronic)).

Pahor, A., & Jausovec, N. (2014). The effects of theta transcranial alternating current stimulation (tACS) on fluid intelligence. *International Journal of Psychophysiology*, *93*(3), 322–331. http://dx.doi.org/10.1016/j.ijpsycho.2014.06.015.

Pascual-Leone, A., & Hallett, M. (1994). Induction of errors in a delayed response task by repetitive transcranial magnetic stimulation of the dorsolateral prefrontal cortex. *Neuroreport*, *5*, 2517–2520 (0959–4965 (Print)).

Pascual-Leone, A., & Pridmore, H. (1995). Transcranial magnetic stimulation (TMS). *The Australian and New Zealand Journal of Psychiatry*, *29*, 698 (0004–8674 (Print)).

Patel, G. H., Yang, D., Jamerson, E. C., Snyder, L. H., Corbetta, M., & Ferrera, V. P. (2015). Functional evolution of new and expanded attention networks in humans. *Proceedings of the National Academy of Sciences of the United States of America*, *112*(30), 9454–9459. http://dx.doi.org/10.1073/pnas.1420395112.

Paul, E. J., Larsen, R. J., Nikolaidis, A., Ward, N., Hillman, C. H., Cohen, N. J., ... Barbey, A. K. (2016). Dissociable brain biomarkers of fluid intelligence. *NeuroImage*, *137*, 201–211. http://dx.doi.org/10.1016/j.neuroimage.2016.05.037 (1095–9572 (Electronic)).

Polania, R., Nitsche, M. A., Korman, C., Batsikadze, G., & Paulus, W. (2012). The importance of timing in segregated theta phase-coupling for cognitive performance. *Current Biology*, *22*, 1314–1318. http://dx.doi.org/10.1016/j.cub.2012.05.021 (1879–0445 (Electronic)).

Postuma, R. B., & Dagher, A. (2006). Basal ganglia functional connectivity based on a meta-analysis of 126 positron emission tomography and functional magnetic resonance imaging publications. *Cerebral Cortex*, *16*(10), 1508–1521. http://dx.doi.org/10.1093/cercor/bhj088.

Prado, J., Van Der Henst, J. B., & Noveck, I. A. (2010). Recomposing a fragmented literature: How conditional and relational arguments engage different neural systems for deductive reasoning. *NeuroImage*, *51*, 1213–1221. http://dx.doi.org/10.1016/j.neuroimage.2010.03.026 (1095–9572 (Electronic)).

Preusse, F., van der Meer, E., Deshpande, G., Krueger, F., & Wartenburger, I. (2011). Fluid intelligence allows flexible recruitment of the parieto-frontal network in analogical reasoning. *Frontiers in Human Neuroscience*, *5*, 22. http://dx.doi.org/10.3389/fnhum.2011.00022 (1662–5161 (Electronic)).

Raichle, M. E. (2015). The brain's default mode network. *Annual Review of Neuroscience*, *38*, 433–447. http://dx.doi.org/10.1146/annurev-neuro-071013-014030 (1545–4126 (Electronic)).

Raven, J., Raven, J. C., & Court, J. H. (1998). *Manual for Raven's progressive matrices and vocabulary scales*.

Reverberi, C., Cherubini, P., Rapisarda, A., Rigamonti, E., Caltagirone, C., Frackowiak, R. S., ... Paulesu, E. (2007). Neural basis of generation of conclusions in elementary

deduction. *NeuroImage*, *38*(4), 752–762. http://dx.doi.org/10.1016/j.neuroimage.2007.07.060.

Reverberi, C., Cherubini, P., Frackowiak, R. S., Caltagirone, C., Paulesu, E., & Macaluso, E. (2010). Conditional and syllogistic deductive tasks dissociate functionally during premise integration. *Human Brain Mapping*, *31*(9), 1430–1445. http://dx.doi.org/10.1002/hbm.20947.

Rhein, C., Muhle, C., Richter-Schmidinger, T., Alexopoulos, P., Doerfler, A., & Kornhuber, J. (2014). Neuroanatomical correlates of intelligence in healthy young adults: The role of basal ganglia volume. *PloS One*, *9*(4), e93623. http://dx.doi.org/10.1371/journal.pone.0093623.

Rorden, C., & Brett, M. (2000). Stereotaxic display of brain lesions. *Behavioural Neurology*, *12*(4), 191–200.

Rueda, M. R., Checa, P., & Combita, L. M. (2012). Enhanced efficiency of the executive attention network after training in preschool children: Immediate changes and effects after two months. *Developmental Cognitive Neuroscience*, (2 Suppl 1), S192–S204. http://dx.doi.org/10.1016/j.dcn.2011.09.004 (1878–9307 (Electronic)).

Ruffini, G., Fox, M. D., Ripolles, O., Miranda, P. C., & Pascual-Leone, A. (2014). Optimization of multifocal transcranial current stimulation for weighted cortical pattern targeting from realistic modeling of electric fields. *NeuroImage*, *89*, 216–225. http://dx.doi.org/10.1016/j.neuroimage.2013.12.002 (1095–9572 (Electronic)).

Santarnecchi, N. R. P., Godone, M., Giovannelli, F., Feurra, M., Matzen, L., Rossi, A., & Rossi, S. (2013). Frequency-dependent enhancement of fluid intelligence induced by transcranial oscillatory potentials. *Current Biology*, *23*(15), 1449–1453. http://dx.doi.org/10.1016/j.cub.2013.06.022.

Santarnecchi, G., Galli, N. R., Polizzotto, Rossi, A., & Rossi, S. (2014). Efficiency of weak brain connections support general cognitive functioning. *Human Brain Mapping*, *35*(9), 4566–4582. http://dx.doi.org/10.1002/hbm.22495.

Santarnecchi, E., Brem, A. K., Levenbaum, E., Thompson, T., Kadosh, R. C., & Pascual-Leone, A. (2015a). Enhancing cognition using transcranial electrical stimulation. *Current Opinion in Behavioural Sciences*, 171–178. no. 1879–0445 (Electronic) (August) http://dx.doi.org/10.1016/j.cub.2013.06.022.

Santarnecchi, Rossi, S., & Rossi, A. (2015b). The smarter, the stronger: Intelligence level correlates with brain resilience to systematic insults. *Cortex*, *64*, 293–309. http://dx.doi.org/10.1016/j.cortex.2014.11.005 (1973–8102 (Electronic)).

Santarnecchi, E., Tatti, E., Rossi, S., Serino, V., & Rossi, A. (2015c). . Intelligence-related differences in the asymmetry of spontaneous cerebral activity. *Human Brain Mapping*, *36*(9), 3586–3602. http://dx.doi.org/10.1002/hbm.22864.

Santarnecchi, T., Muller, S., Rossi, A., Sarkar, N. R., Polizzotto, A. R., & Cohen Kadosh, R. (2016). Individual differences and specificity of prefrontal gamma frequency-tACS on fluid intelligence capabilities. *Cortex*, *75*(February), 33–43. http://dx.doi.org/10.1016/j.cortex.2015.11.003.

Schlagenhauf, F., Rapp, M. A., Huys, Q. J., Beck, A., Wustenberg, T., Deserno, L., Buchholz, H. G., et al. (2013). Ventral striatal prediction error signaling is associated with dopamine synthesis capacity and fluid intelligence. *Human Brain Mapping*, *34*(6), 1490–1499. http://dx.doi.org/10.1002/hbm.22000.

Sela, T., Kilim, A., & Lavidor, M. (2012). Transcranial alternating current stimulation increases risk-taking behavior in the balloon analog risk task. *Frontiers in Neuroscience*, *6*, 22. http://dx.doi.org/10.3389/fnins.2012.00022 (1662–453X (Electronic)).

Shirer, W. R., Ryali, S., Rykhlevskaia, E., Menon, V., & Greicius, M. D. (2012). Decoding subject-driven cognitive States with whole-brain connectivity patterns. *Cerebral Cortex*, *22*(1), 158–165. http://dx.doi.org/10.1093/cercor/bhr099.

Simard, I., Luck, D., Mottron, L., Zeffiro, T. A., & Soulieres, I. (2015). Autistic fluid intelligence: Increased reliance on visual functional connectivity with diminished modulation of coupling by task difficulty. *Neuroimage. Clin. 9*, 467–478. http://dx.doi.org/10.1016/j.nicl.2015.09.007 (2213–1582 (Electronic)).

Snowball, A., Tachtsidis, I., Popescu, T., Thompson, J., Delazer, M., Zamarian, L., ... Cohen, K. R. (2013). Long-term enhancement of brain function and cognition using cognitive training and brain stimulation. *Current Biology*. no. 1879–0445 (Electronic) (May) http://dx.doi.org/10.1016/j.cub.2013.04.045.

Sporns, O. (2013). Network attributes for segregation and integration in the human brain. *Current Opinion in Neurobiology*. no. 1873–6882 (Electronic) (January) http://dx.doi.org/10.1016/j.conb.2012.11.015.

Sprugnoli, G., Rossi, S., Emmerdorfer, A., Rossi, A., Liew, S.-L., Tatti, E., ... Santarnecchi, E. (2017). Neural correlates of eureka moment. *Intelligence*. http://dx.doi.org/10.1016/j.intell.2017.03.004 (March).

Tatti, E., Rossi, S., Innocenti, I., Rossi, A., & Santarnecchi, E. (2016). Non-invasive brain stimulation of the aging brain: State of the art and future perspectives. *Ageing Research Reviews*, *29*, 66–89. http://dx.doi.org/10.1016/j.arr.2016.05.006 (1872–9649 (Electronic)).

Tavor, I., Parker, J. O., Mars, R. B., Smith, S. M., Behrens, T. E., & Jbabdi, S. (2016). Task-free MRI predicts individual differences in brain activity during task performance. *Science*, *352*(6282), 216–220. http://dx.doi.org/10.1126/science.aad8127.

Thut, G., Nietzel, A., & Pascual-Leone, A. (2005). Dorsal posterior parietal rTMS affects voluntary orienting of visuospatial attention. *Cerebral Cortex*, *15*(5), 628–638. http://dx.doi.org/10.1093/cercor/bhh164.

Thut, G., Miniussi, C., & Gross, J. (2012). The functional importance of rhythmic activity in the brain. *Current Biology*, *22*(16), R658–R663. http://dx.doi.org/10.1016/j.cub.2012.06.061.

Turkeltaub, P. E., Eickhoff, S. B., Laird, A. R., Fox, M., Wiener, M., & Fox, P. (2012). Minimizing within-experiment and within-group effects in activation likelihood estimation meta-analyses. *Human Brain Mapping*, *33*, 1–13. http://dx.doi.org/10.1002/hbm.21186 (1097–0193 (Electronic)).

Unsworth, N., Spillers, G. J., & Brewer, G. A. (2010). The contributions of primary and secondary memory to working memory capacity: An individual differences analysis of immediate free recall. *Journal of Experimental Psychology: Learning, Memory, and Cognition*, *36*(1), 240–247. http://dx.doi.org/10.1037/a0017739.

Vakhtin, A. A., Ryman, S. G., Flores, R. A., & Jung, R. E. (2014). Functional brain networks contributing to the parieto-frontal integration theory of intelligence. *NeuroImage*, *103*(December), 349–354. http://dx.doi.org/10.1016/j.neuroimage.2014.09.055.

Wang, J. X., Rogers, L. M., Gross, E. Z., Ryals, A. J., Dokucu, M. E., Brandstatt, K. L., ... Voss, J. L. (2014). Targeted enhancement of cortical-hippocampal brain networks and associative memory. *Science*, *345*(6200), 1054–1057. http://dx.doi.org/10.1126/science.1252900.

Wartenburger, I., Heekeren, H. R., Preusse, F., Kramer, J., & van der Meer, E. (2009). Cerebral correlates of analogical processing and their modulation by training. *NeuroImage*, *48*(1), 291–302. http://dx.doi.org/10.1016/j.neuroimage.2009.06.025.

Whalley, L. J., Deary, I. J., Appleton, C. L., & Starr, J. M. (2004). Cognitive reserve and the neurobiology of cognitive aging. *Ageing Research Reviews*, *3*(4), 369–382. http://dx.doi.org/10.1016/j.arr.2004.05.001.

Woldorff, M. G., Hazlett, C. J., Fichtenholtz, H. M., Weissman, D. H., Dale, A. M., & Song, A. W. (2004). Functional Parcellation of attentional control regions of the brain. *Journal of Cognitive Neuroscience*, *16*(1), 149–165. http://dx.doi.org/10.1162/089892904322755638.

Yeo, B. T., Krienen, F. M., Sepulcre, J., Sabuncu, M. R., Lashkari, D., Hollinshead, M., Roffman, J. L., et al. (2011). The organization of the human cerebral cortex estimated by intrinsic functional connectivity. *Journal of Neurophysiology*, *106*(3), 1125–1165. http://dx.doi.org/10.1152/jn.00338.2011.

Yuan, Z., Qin, W., Wang, D., Jiang, T., Zhang, Y., & Yu, C. (2012). The salience network contributes to an Individual's fluid reasoning capacity. *Behavioural Brain Research*, *229*(2), 384–390. http://dx.doi.org/10.1016/j.bbr.2012.01.037.